

AD No. / 5523

ASTIA FILE COPY

# Magnetic and Electric Properties of Magnetite at Low Temperatures

Technical Report 68  
Laboratory for Insulation Research  
Massachusetts Institute of Technology

July, 1953

**Magnetic and Electric Properties of Magnetite  
at Low Temperatures**

by

**B. A. Calhoun**

**Laboratory for Insulation Research  
Massachusetts Institute of Technology  
Cambridge, Massachusetts**

**MAGNETIC AND ELECTRIC PROPERTIES OF MAGNETITE**  
**AT LOW TEMPERATURES**

by

B. A. Calhoun

Laboratory for Insulation Research  
Massachusetts Institute of Technology  
Cambridge, Massachusetts

**Abstract:** Verwey has suggested that the low temperature transition in magnetite is due to the ordering of the ferrous and ferric ions in the octahedral interstices of the spinel lattice and has proposed a specific ordered structure. This arrangement would require that the crystal symmetry changes from cubic to orthorhombic. X-ray diffraction, electric conductivity and magnetization measurements confirm that the transition leads to an orthorhombic structure. The c axis of this orthorhombic structure is established along the cube edge closest to the direction of magnetization in each domain. An external magnetic field applied to a crystal of magnetite, as it is cooled through the transition, establishes a preferred orientation for the c axis throughout the whole crystal by aligning the domains above the transition. The application of a sufficiently strong magnetic field below the transition can cause this c axis to switch to a new direction. This process involves a co-operative rearrangement of the ferrous ions in new sites, and is accompanied by relatively large changes in dimensions. In stoichiometric, synthetic, single crystals the transition occurs at  $119.4^{\circ}\text{K}$  and is marked by an abrupt decrease in the conductivity by a factor of 90 in a temperature interval of  $1^{\circ}$ . No thermal hysteresis is observed. The conductivity of a

crystal cooled through the transition in a strong magnetic field is anisotropic below the transition. It can be represented by the equation  $\sigma = A + B(1 + \cos^2 \theta)$ , where  $\theta$  is the angle between the c axis and the direction of measurement. The ratio  $B/(A + B)$  increases rapidly as the crystal is cooled from the transition to  $90^\circ\text{K}$ , indicating a progressive increase in the long-range order. The magnetic anisotropy energy below the transition has the form consistent with orthorhombic holohedral symmetry. The c axis is the direction of easy magnetization below the transition, and the anisotropy energy is very much larger below than above. The anisotropy constants have been determined at  $85^\circ\text{K}$  from measurements of the areas between the magnetization curves in different crystallographic orientations. If the orthorhombic axes are differently oriented in different regions of the crystal, the magnetic behavior of magnetite becomes still more complicated.

Magnetite has been intensively studied in this laboratory in recent years, both as a prototype of the ferrites and because of its unusual behavior at low temperatures (from  $-140^\circ$  to  $-190^\circ\text{C}$ ).<sup>1, 2)</sup> The initial permeability passes through a maximum at ca.  $-140^\circ\text{C}$  and then decreases rapidly to a very small value below  $-155^\circ\text{C}$ . Bickford<sup>1)</sup> has shown that this maximum is due to the vanishing of the crystalline anisotropy energy. At ca.  $-155^\circ\text{C}$  a transition is observed. The specific heat traverses a maximum;<sup>3)</sup> the electrical conductivity decreases by a factor of ca. 100;<sup>4)</sup> and the material is much harder to magnetize to saturation

1) L. R. Bickford, Jr., Tech. Rep. 23; Phys. Rev. 78, 449 (1950).

2) C. A. Domenicali, Tech. Rep. 25; Phys. Rev. 78, 458 (1950).

3) R. W. Millar, J. Am. Chem. Soc. 51, 215 (1929).

4) E. J. W. Verwey, Nature 144, 327 (1939); E. J. W. Verwey and P. W. Haayman, Physica 3, 979 (1941).

below the transition.<sup>5)</sup> The direction of easy magnetization below the transition is influenced by a magnetic field applied as the sample is cooled through the transition.<sup>6)</sup>

Verwey<sup>4)</sup> proposed that above the transition magnetite has the inverse spinel structure, and that the transition itself is due to an ordering of the random distribution of ferrous and ferric ions which occupy the octahedral interstices in the crystal. The ordered arrangement shown in Fig. 1 appeared to him as the most likely one.<sup>7)</sup> Verwey suggested that the c axis of this ordered structure would lie along the cube edge closest to the direction of the external field applied during cooling through the transition.

The object of the present research was to study this unusual type of transition by X-ray analysis as well as by electric and magnetic means. This investigation was undertaken on the single crystals of magnetite grown by Smiltens<sup>8)</sup> in this laboratory.

### CRYSTAL STRUCTURE

The ferrites have the same crystal structure as spinel ( $\text{MgOAl}_2\text{O}_3$ ). The unit cell of the structure contains 32 oxygen ions in an almost cubic close-packed arrangement. The metallic ions occupy two types of interstices in this oxygen lattice: 8 tetrahedral and 16 octahedral. In simple ferrites two variations can occur. In those with a normal spinel structure, one kind of ion occupies each type of site. In the inverse spinel structure, the octahedral interstices are occupied by two kinds of cations, distributed at random over the 16 sites.

5) P. Weiss and R. Forrer, Ann. phys. [10] 12, 279 (1929).

6) C. H. Li, Phys. Rev. 40, 1002 (1932).

7) E. J. Verwey, P. W. Haayman and F. C. Romeijn, J. Chem. Phys. 15, 181 (1947).

8) J. Smiltens, Tech. Rep. 49; J. Chem. Phys. 20, 990 (1952).

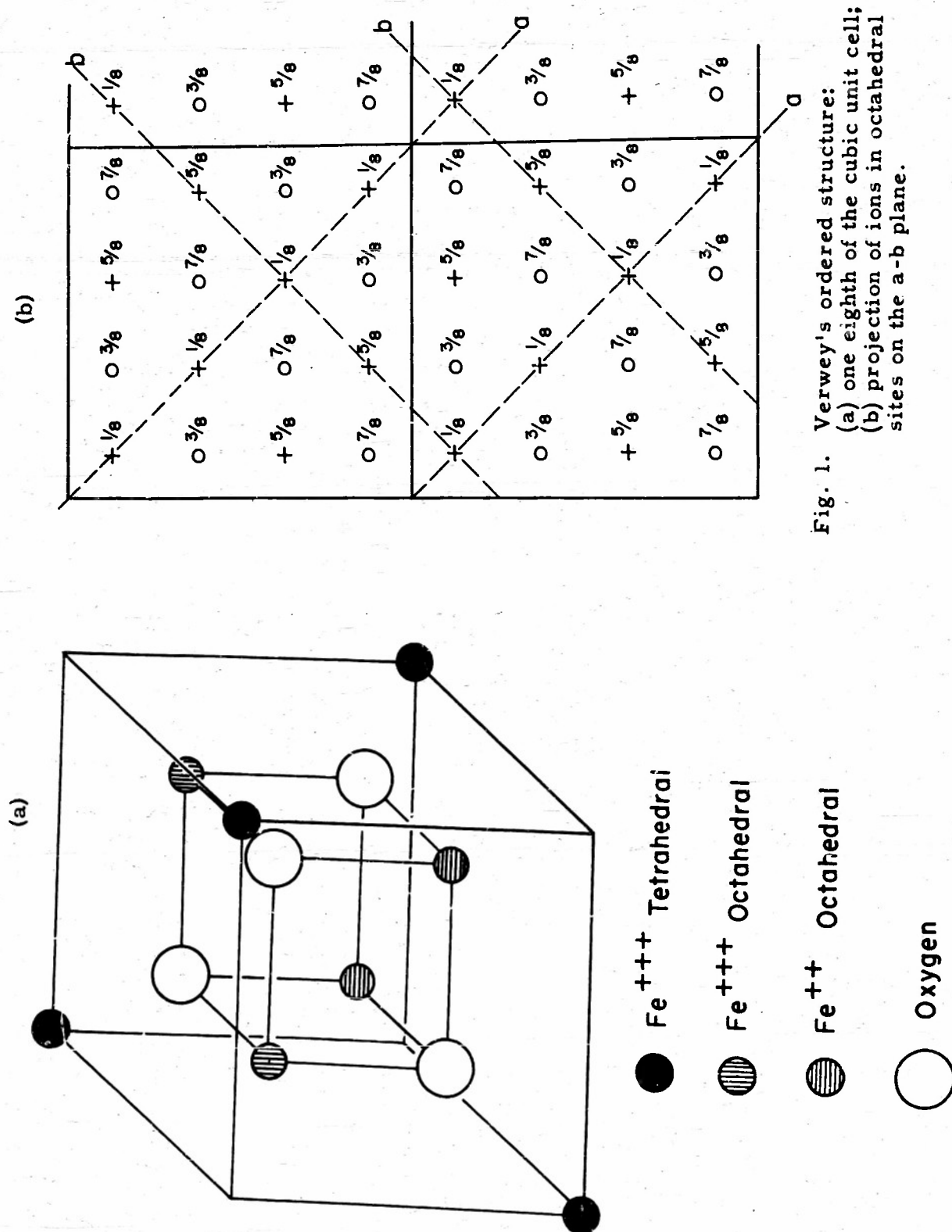


Fig. 1. Verwey's ordered structure:  
(a) one eighth of the cubic unit cell;  
(b) projection of ions in octahedral sites on the a-b plane.

Neutron diffraction measurements have established that magnetite has the inverse structure.<sup>9)</sup>

An X-ray investigation, the details of which have been published elsewhere,<sup>10)</sup> showed that the symmetry of magnetite below the transition is orthorhombic, with unit cell dimensions:  $a = 5.912$ ,  $b = 5.945$ ,  $c = 8.388\text{\AA}$  at  $78^\circ\text{K}$ . The  $c$  axis lies along one of the original cube edges, and the  $a$  and  $b$  axes lie along the face diagonals normal to the  $c$  axis. These results are in agreement with those obtained by Bickford<sup>11)</sup> from measurements of the deformations of single crystals on cooling through the transition. This is also the unit cell that would be expected on the basis of the ordered arrangement of Fig. 1.

#### ESTABLISHMENT OF THE MAGNETIC AXIS

The orthorhombic axes can have any of six possible orientations relative to the cubic axes. In the absence of any external conditions to make one or more of these orientations preferred, they should all occur in approximately equal amounts. The effect of a magnetic field in making one or more of these orientations preferred was studied using the null-coil pendulum magnetometer developed in this laboratory by Domenicali.<sup>12)</sup> Some modifications were made in the magnetometer to permit its use down to liquid helium temperatures. The case of the instrument was evacuated and helium gas, admitted through a needle valve, was used to regulate the rate of warming by controlling the heat loss from the sample. The sample was mounted in an aluminum boat in good thermal contact with the null coil, which also served as a heat source. The measurements were made on a circular disk cut from a (100)-plane slice of a single crystal of

9) C. G. Shull, E. O. Wollan and W. C. Koehler, Phys. Rev. **84**, 912 (1951).

10) S. C. Abrahams and B. A. Calhoun, Tech. Rep. 61.

11) L. R. Bickford, Jr., Revs. Mod. Phys. **25**, 75 (1953).

12) C. A. Domenicali, Tech. Rep. 24; Rev. Sci. Inst. **21**, 327 (1950).

magnetite. The edges of this disk were ground by hand until it was approximately an oblate spheroid with axes of 4.55 and 0.89 mm.

The smallest magnetic field that sufficed to establish the magnetic axis was determined by cooling the (100) sample through the transition with magnetic fields of various strengths applied parallel to the [001] direction. The sample was then demagnetized and the magnetization curve in the [001] direction measured at  $-195^{\circ}\text{C}$ . From the curves shown in Fig. 2 it was clear that the minimum field necessary to completely establish the magnetic axis is ca. 1000 oersteds, and that this is approximately the same field needed to produce technical saturation. The magnetic axis is established along the cube edge nearest the direction of magnetization in each domain. The function of the external field is to align the individual domains so that throughout the sample there will be a unique magnetic axis. It is obvious that this magnetic axis must be the c axis of the orthorhombic structure.

When a sample, which has been cooled in a field to establish the c axis throughout in the same direction, is demagnetized the c axis is the direction of easy magnetization and the domain pattern in the demagnetized state will consist of antiparallel domains aligned along the c axis. This was verified by measuring the longitudinal magnetostriction (see Appendix 2) in the [100] bar after cooling through the transition in a field parallel to its length and then demagnetizing the bar. The longitudinal magnetostriction in fields up to ca. 10,000 oersteds was extremely small ( $\delta l/l < 10^{-6}$ ) indicating that the magnetization in this direction was almost entirely due to the motion of  $180^{\circ}$  walls.

In additional experiments the (100) sample was cooled through the transition in a field of 4700 oersteds, directed in the (100) plane at angles of  $0^{\circ}$ ,  $40^{\circ}$ ,  $45^{\circ}$ ,  $55^{\circ}$ , and  $90^{\circ}$  to the [001] direction. The warming curves (magnetic moment as a function of temperature at constant applied field) are shown in Figs. 3 to 5. When the field is within  $40^{\circ}$  of the [001] direction, this [001] becomes the c axis.

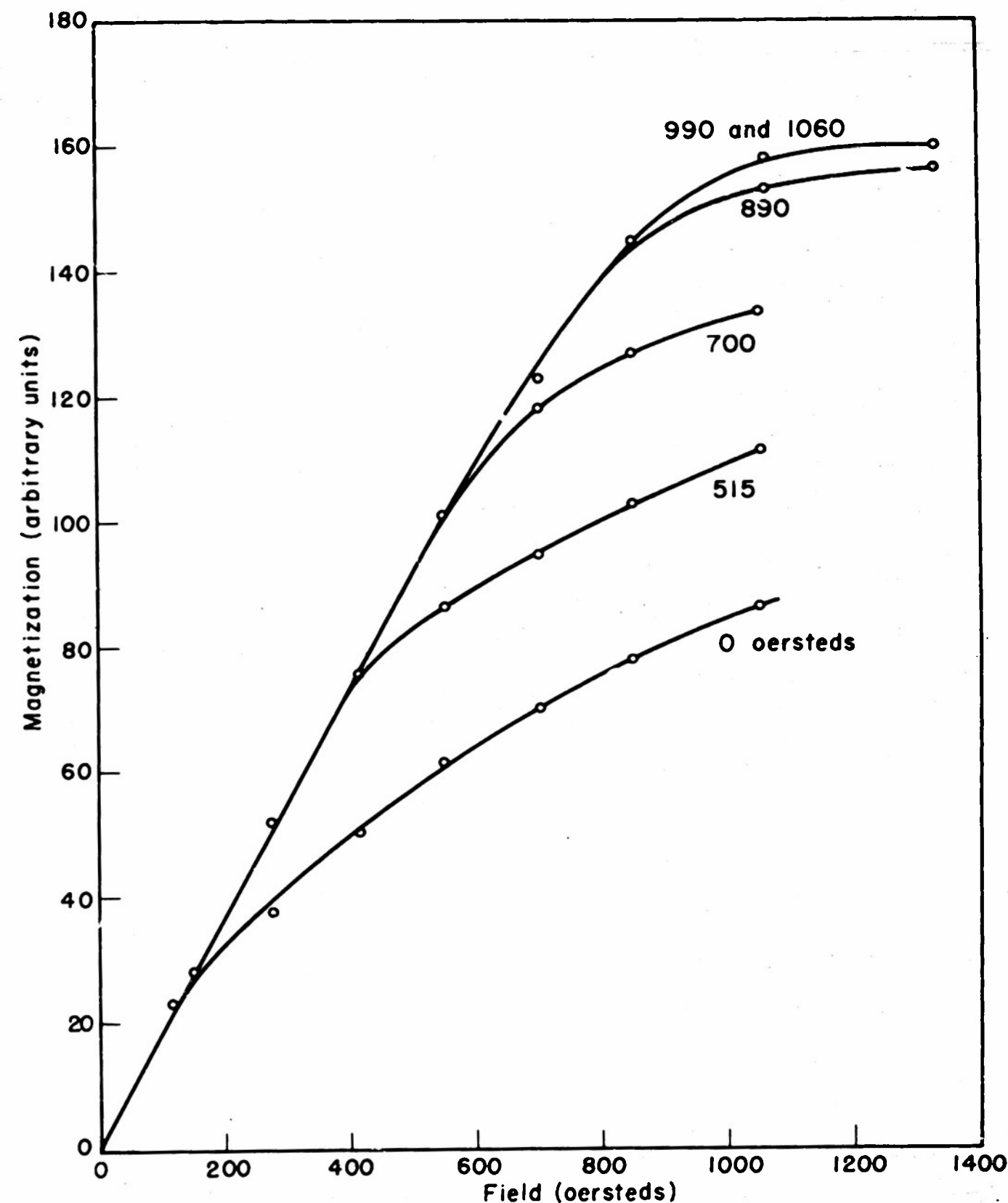


Fig. 2. Magnetization curves in the cubic [001] direction at  $78^{\circ}\text{K}$  after cooling with the indicated fields parallel to [001].

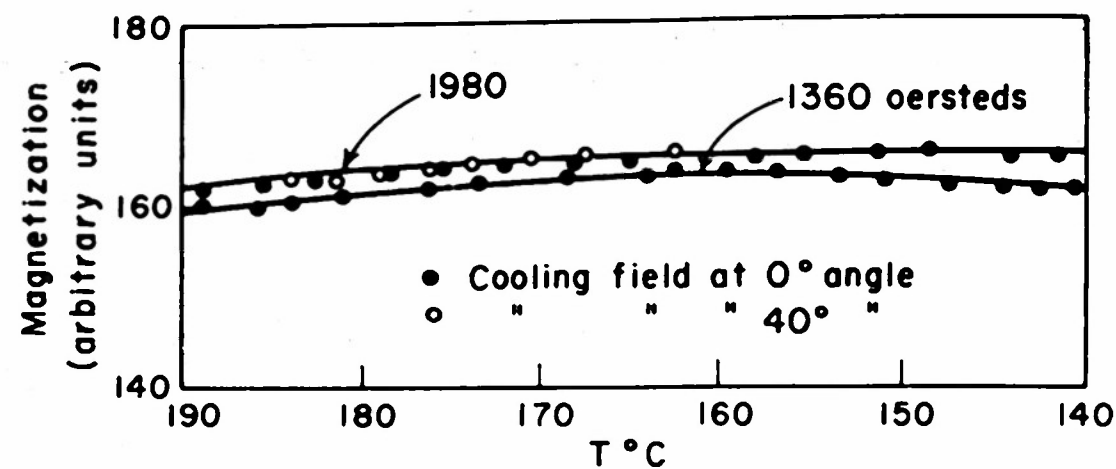


Fig. 3. Warming curves in  $[001]$  direction after cooling with a field of 4700 oersteds at  $0^\circ$  and  $40^\circ$  to  $[001]$ .

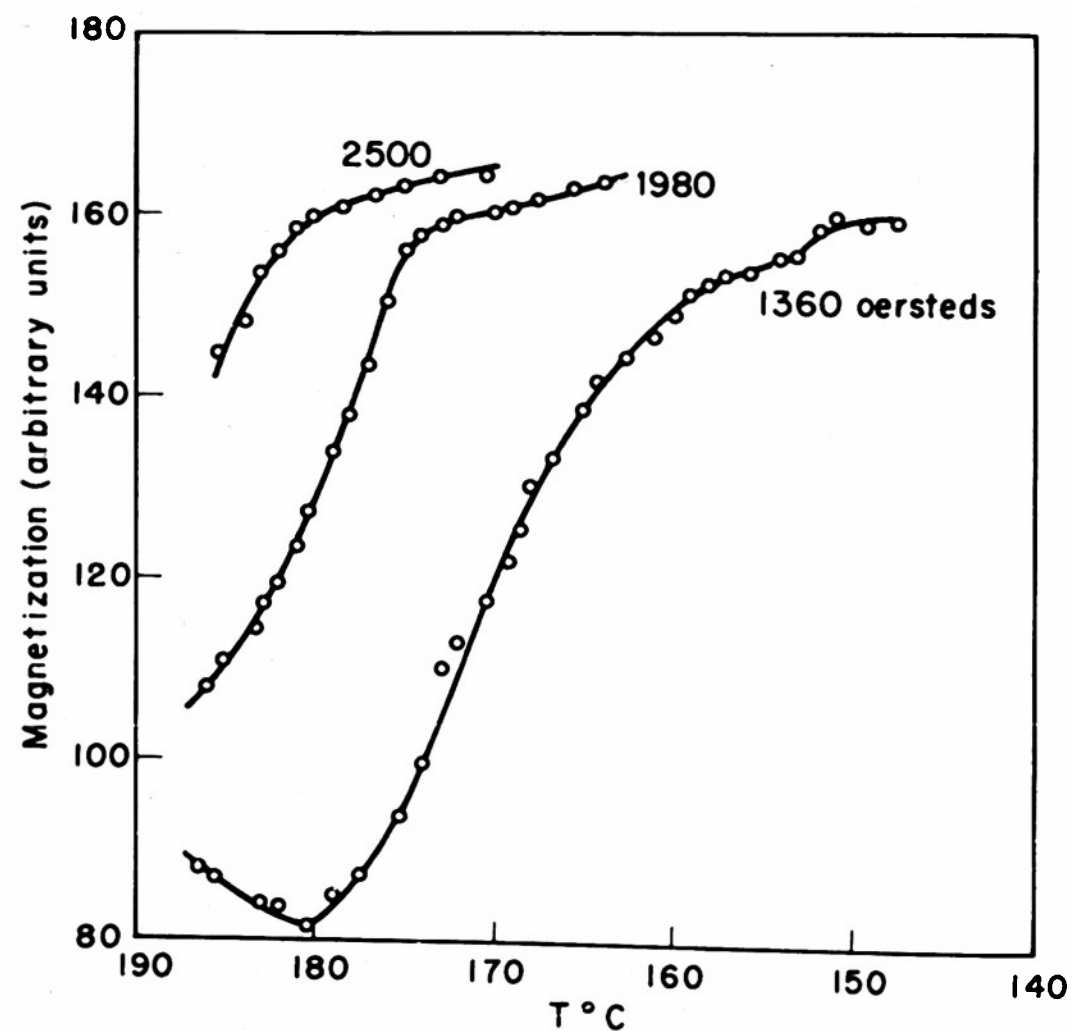


Fig. 4. Warming curves in  $[001]$  direction after cooling with a field of 4700 oersteds at  $45^\circ$  to  $[001]$ .

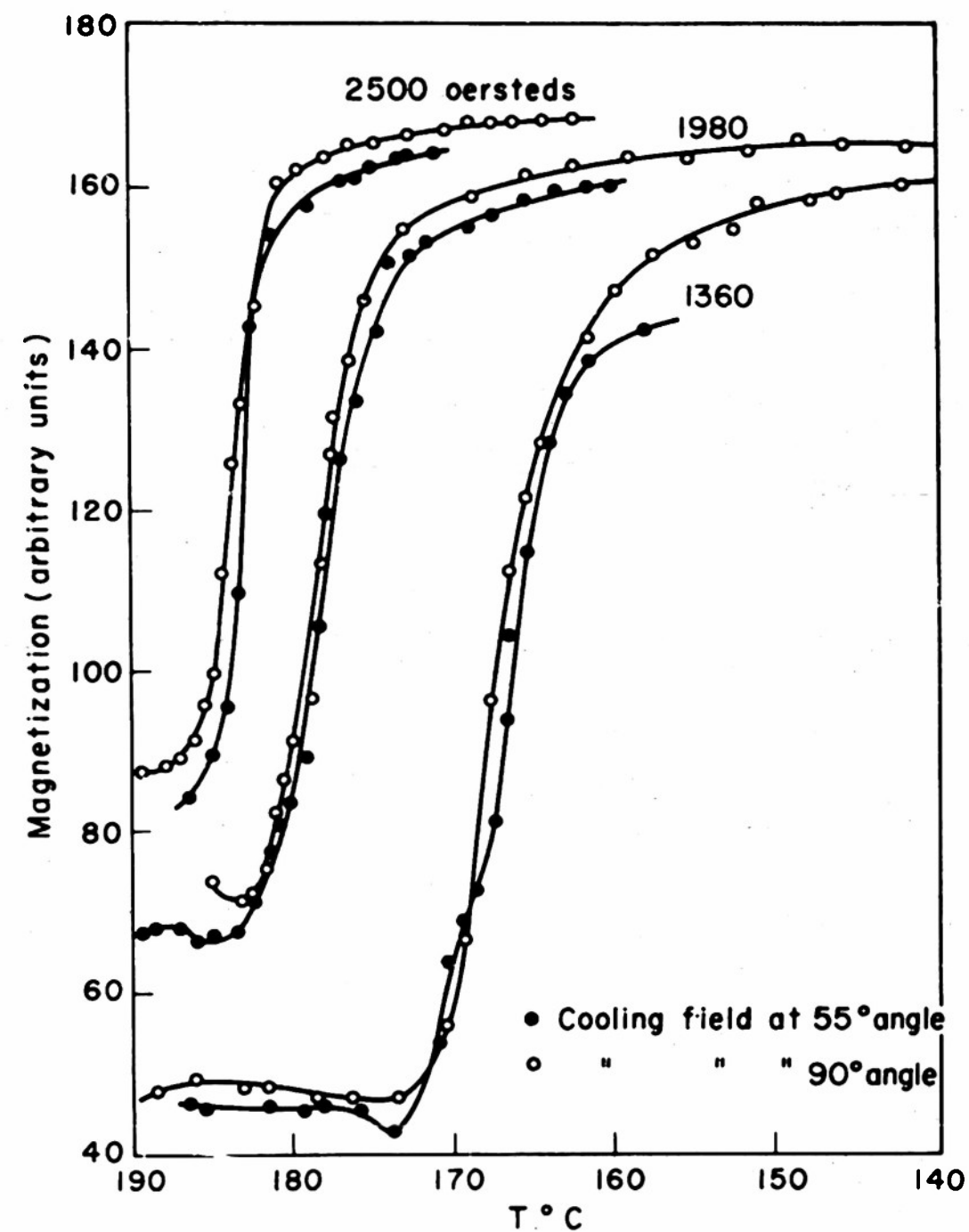


Fig. 5. Warming curves in  $[001]$  direction after cooling with a field of 4700 oersteds at  $55^\circ$  and  $90^\circ$  to  $[001]$ .



When the field is within  $40^\circ$  of the  $[010]$  direction, i.e., more than  $50^\circ$  from  $[001]$ ,  $[010]$  becomes the c axis and the  $[001]$  direction is magnetically hard. When the cooling field is applied at  $45^\circ$  to  $[001]$ , the warming curves show that in approximately one half the sample  $[001]$  is the c axis and in the remainder  $[010]$  is the c axis.

The effect of applying a magnetic field at various angles in the cubic (110) plane was investigated, using the quasi-static B-H loop tracer (see below) and an oblate spheroidal sample prepared from a (110) slice of a magnetite crystal. Magnetization curves were measured in the  $[001]$  direction of this sample, after cooling in a field of 10,000 oersteds directed in the (110) plane at angles of  $0^\circ$ ,  $25^\circ$ , and  $40^\circ$  to  $[001]$ . The identity of the curves shows that, in each case, the c axis is established along the  $[001]$  direction. All these results are consistent with the picture that the c axis is established along the cube edge nearest the direction of the magnetization in each domain. Generally similar results have been obtained recently with natural crystals of magnetite by Williams and Bozorth.<sup>13)</sup>

#### SWITCHING OF THE MAGNETIC AXIS

The phenomenon of axis switching, i.e., the change of the c axis from one cube edge to another below the transition, was first observed by Bickford<sup>1)</sup> in the microwave resonance experiments at liquid nitrogen temperature. The effect is apparent in the warming curves shown in Fig. 5. The magnetic axis was established along the  $[010]$  direction so that  $[001]$  was magnetically hard, as shown by its small magnetic moment. Then, at some temperature below the transition, there is an abrupt increase in the magnetic moment indicating that the  $[001]$  direction has suddenly become an easy direction. This effect is

13) H. J. Williams and R. M. Bozorth, Revs. Mod. Phys. 25, 79 (1953).

of considerable importance for two reasons. Obviously it must be considered in interpreting experimental results and also in planning experiments, since some measurements which appear to be straightforward are impossible except at very low temperatures. It also provides an additional means of obtaining information about the energies involved in the transition. The temperature at which this change occurs depends on the external field applied parallel to the  $[001]$  direction. The external field necessary to cause axis-switching at various temperatures was determined by cooling the (100) spheroid through the transition with a field of 4700 oersteds along the  $[010]$  direction and then measuring the warming curves with applied fields of from 1000 to 5000 oersteds. A number of these curves are shown in Fig. 6.

Axis switching was also observed in certain directions in the (110) plane. Figure 7 shows the magnetization curves observed in the  $[1\bar{1}0]$  direction after cooling in a field of 10,000 oersteds parallel or perpendicular (in the (110) plane) to this direction. An unexpected result is that axis-switching occurred only in the  $[1\bar{1}0]$  direction and in a direction at  $15^\circ$  to it. From measurements of the change in length of a  $[100]$  bar (see Appendix 2) accompanying the axis switching, it was evident that relatively large changes in dimensions ( $\delta l/l \sim 10^{-4}$ ) and hence in elastic energy are involved in this process. This elastic energy apparently suffices, in the case just mentioned, to prevent the axis-switching from occurring at the field indicated by Eq. (2), although it may still occur in a sufficiently high field.

Transfer of the c axis from one cube edge to another requires that electrons jump from ferrous to neighboring ferric ions in the tetrahedra formed by the iron ions in the octahedral interstices (cf. Fig. 1). A crystal in which the c axis has been established along the  $[010]$  direction, placed in a magnetic field directed along the  $[001]$  direction, could reduce its energy considerably



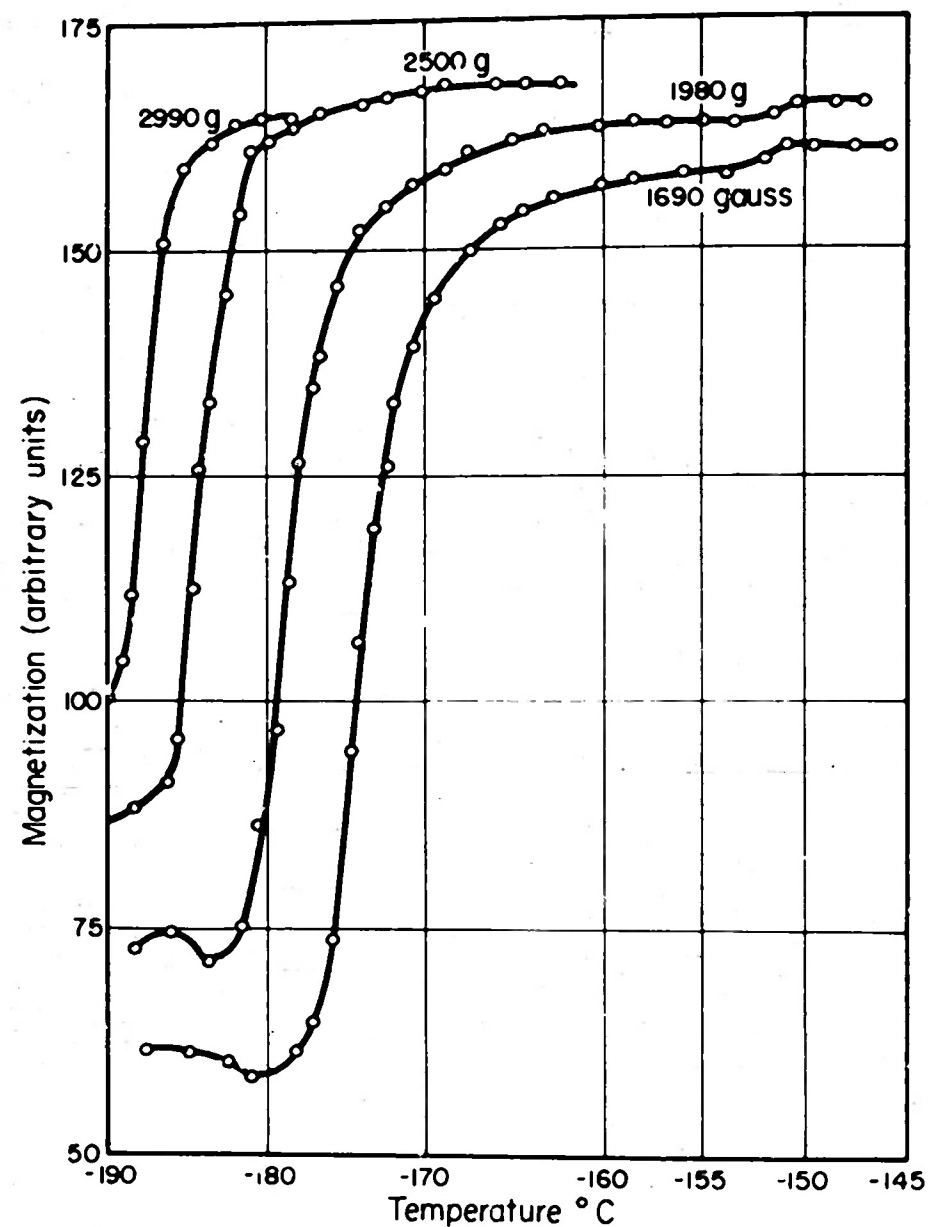


Fig. 6. Warming curves, 100 direction.

if  $[001]$  became the easy direction. The dependence of this energy difference on the magnetic induction is complicated since it is determined by the anisotropy energy.

At present, we will be content with a statistical approach to this problem.

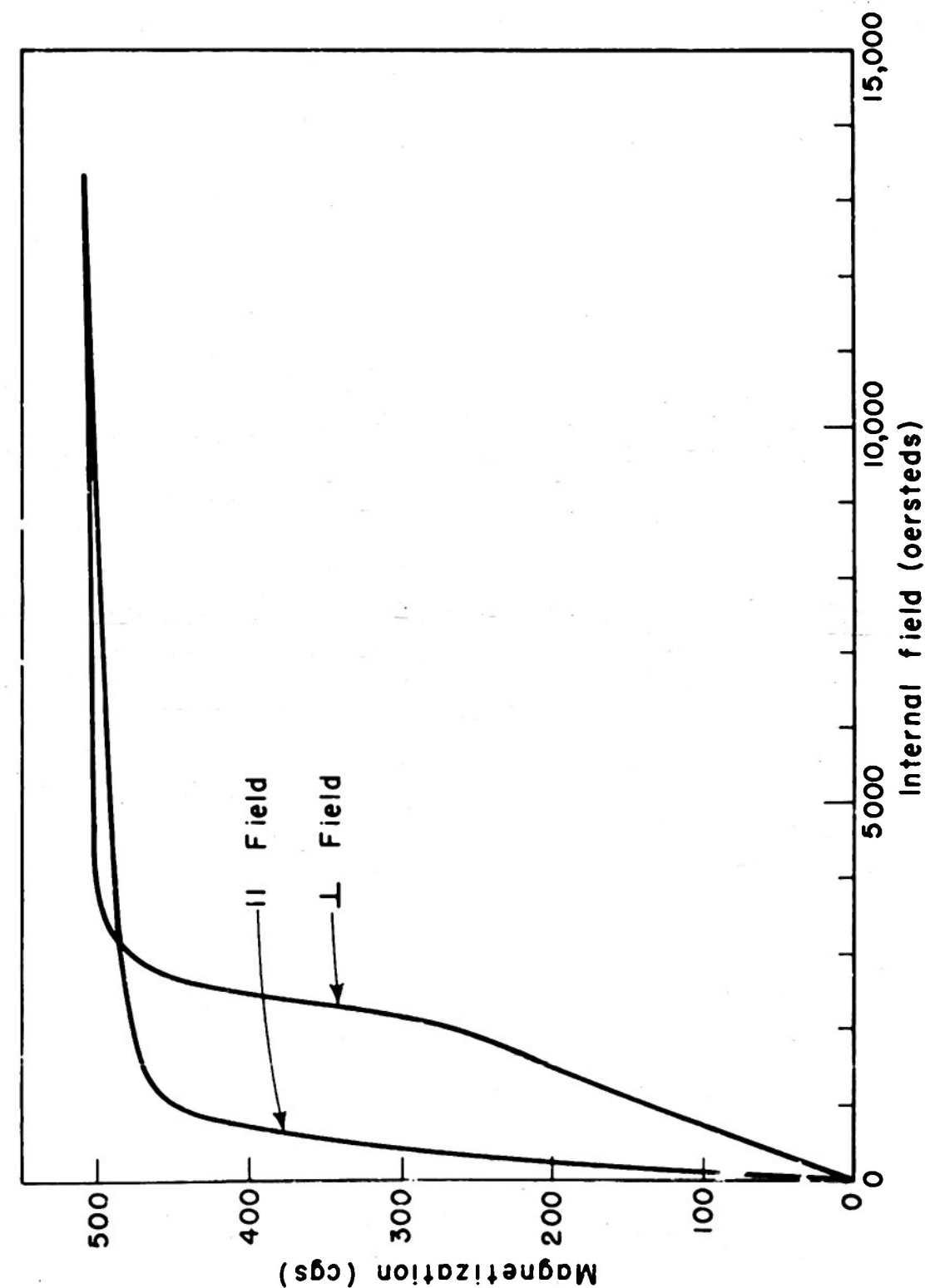


Fig. 7. Magnetization curves at  $85^{\circ}\text{K}$  in the  $[110]$  direction of a  $(110)$  plane after cooling with a field of 10,000 oersteds at an angle of  $0^{\circ}$  and  $90^{\circ}$  to  $[110]$ .

We consider an electron and its two possible positions, an "a" site corresponding to the c axis in the  $[010]$  direction and a "b" site corresponding to the c axis in the  $[001]$  direction. Initially, there is a high probability that an electron will be at an "a" site, since the process of cooling the crystal in a field directed along  $[010]$  slightly lowered the energy of the "a" site relative to that of the "b" site. The application of a magnetic field in the  $[001]$  direction lowers the energy of site "b". We will assume that the change in the energy of the "b" sites is proportional to the internal magnetic induction. The net probability that an electron will jump from an "a" to a "b" site is then given by the expression

$$\exp(-u/kT) (1 - \exp[-\mu B_i/kT]) = \frac{\mu B_i}{kT} \exp(-u/kT), \quad (1)$$

where  $\mu B_i$  is the energy difference between sites "a" and "b" due to the magnetic field. In writing this expression, we have assumed that the initial energy difference between the "a" and "b" sites is small compared to  $\mu B_i$ . We have so far neglected the effects of the local disordering which accompanies a jump from an "a" to a "b" site. This disordering would raise the energy of an electron in the "b" site and hence we may expect an electron would return to an "a" site unless some of its neighbors also jumped to "b" sites before it had time to return. We may say crudely that the net probability (Eq. 1) must be equal to some fixed value before the "b" sites become stable and the axis switches.

Thus we can write the relation between the magnetic induction and the temperature at which the c axis switches as

$$B_i = CT(\exp u/kT) \quad (2)$$

where  $B_i$  is the internal induction prior to the axis-switching and T is the temperature at the mid-point of the switching. Figure 8 shows the experimental data calculated from the curves shown in Fig. 6. It is clear that the data fits the above equation with  $u = 0.033$  ev.

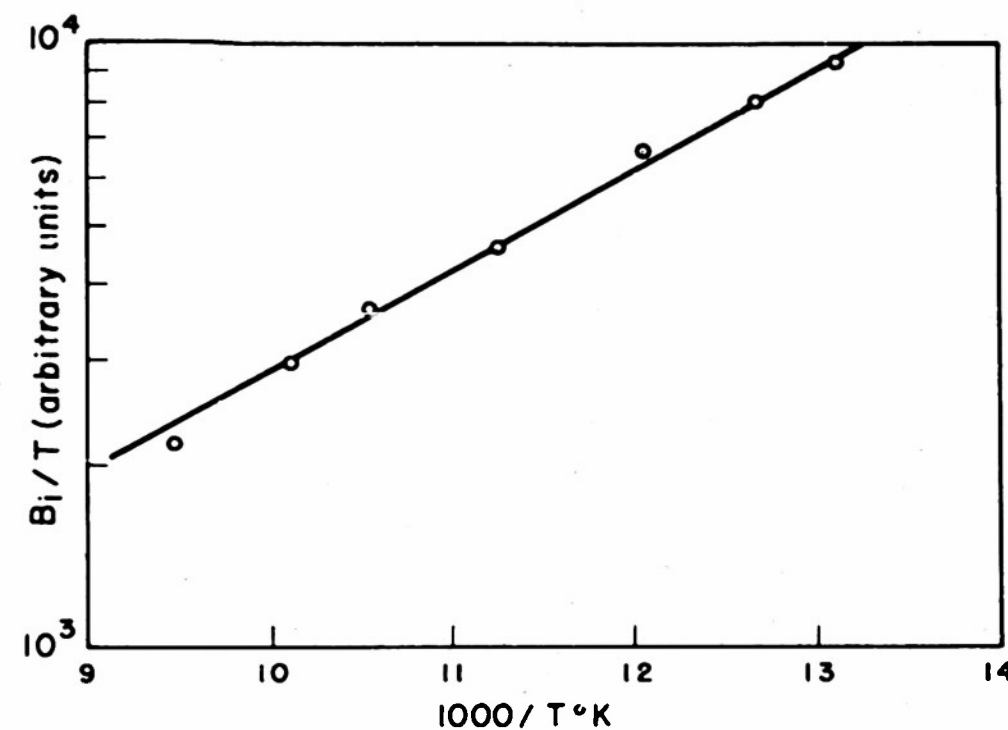


Fig. 8. Induction necessary to switch the c axis.

#### CONDUCTIVITY OF MAGNETITE AND ITS RELATION TO THE TRANSITION

If the conductivity of magnetite is due to the exchange of electrons between the ferrous and ferric ions in the octahedral lattice sites, we would expect the random distribution above the transition to cause isotropic conductivity but below the transition the conductivity should be anisotropic (cf. Fig. 13). This anisotropy and its dependence on both crystallographic orientation and the direction of a magnetic field during cooling have been studied in detail. The conductivity was measured by the usual four-terminal method. The sample holder (Fig. 9) was designed to maintain the sample and the contacts in as nearly as possible an isothermal region in order to minimize spurious thermal emfs. The temperature was measured using a copper-constantan thermocouple and a potentiometer similar

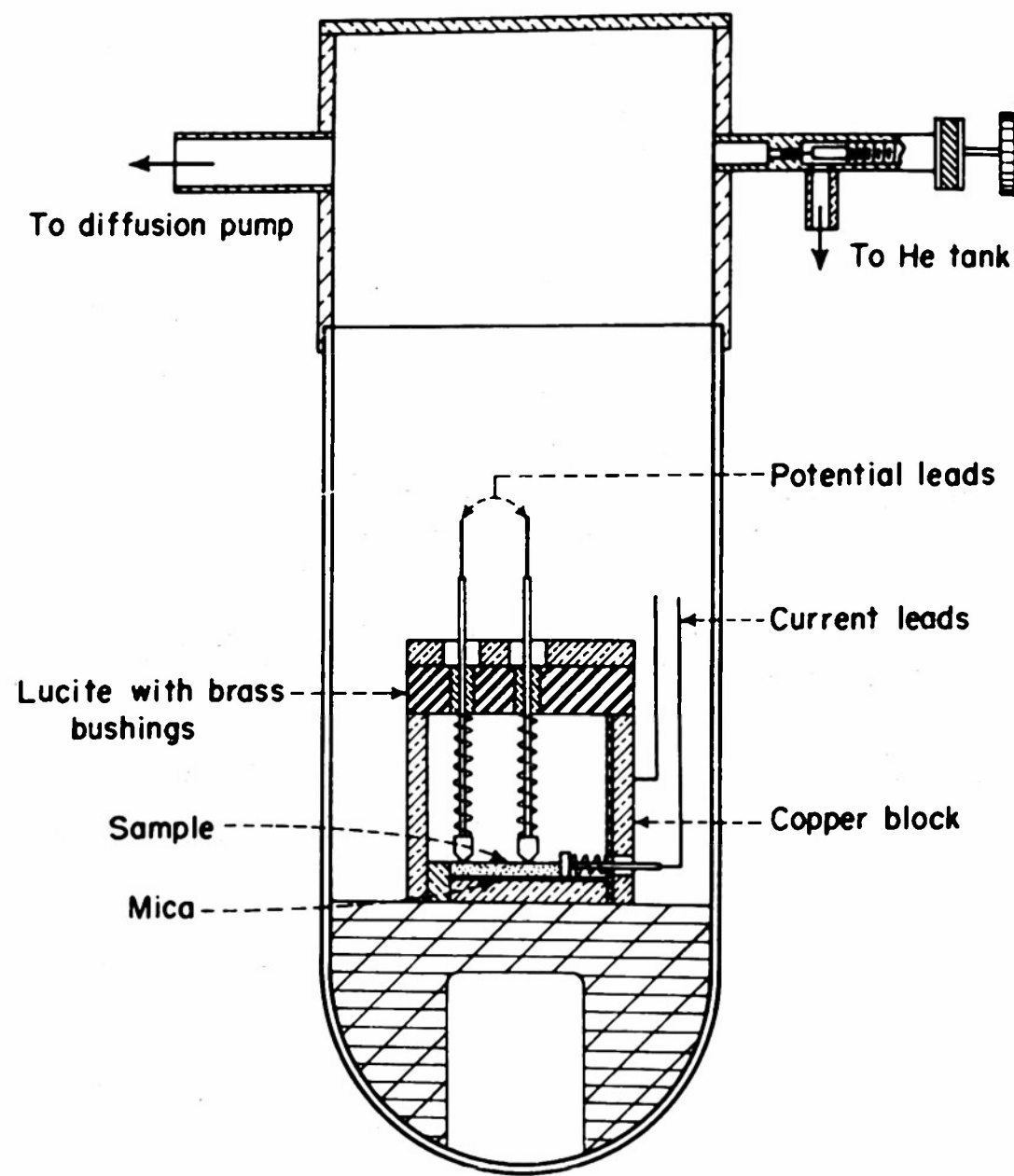


Fig. 9. Conductivity sample holder.

to one described by Teele and Schuhmann.<sup>14)</sup> The sample holder was mounted in an evacuated glass tube. Helium gas, admitted through a needle valve, allowed the pressure to be varied from  $10^{-2}$  to  $10^{-5}$  mm and consequently the warming and cooling rates could be controlled from  $3^{\circ}$  to  $50^{\circ}\text{C}$  per hour. The samples used were cut from two synthetic crystals in the form of rectangular bars about 1 cm in length and with a cross-sectional area of about 3 sq. mm. The length of the bar was parallel to the cubic  $[100]$ ,  $[110]$ , and  $[111]$  directions, respectively.

The conductivity of two of the specimens between room temperature and the transition is shown in Fig. 10. The data, taken during warming as well as cooling cycles, coincide; there was no thermal hysteresis connected with the transition. The conductivity is  $250 \text{ ohm}^{-1} \text{ cm}^{-1}$  at room temperature and has a very broad maximum at ca.  $15^{\circ}\text{C}$ , which does not show clearly in the figure. Previous investigators<sup>2, 4)</sup> have reported this maximum at a somewhat higher temperature (ca.  $80^{\circ}\text{C}$ ). The transition is marked by a decrease of a factor of 90 in the conductivity in a temperature interval of ca.  $1^{\circ}$ . The midpoint of this interval occurred at a temperature of  $119.4 \pm 0.3^{\circ}\text{K}$  ( $-153.8^{\circ}\text{C}$ ).

The conductivity below the transition for samples cooled in zero magnetic field is isotropic (Figs. 11 and 12) but does not follow a simple exponential law

$$\sigma = A \exp(-u/kT)$$

If fitted to this type of law over certain ranges of temperature, one obtains the values of the constants  $A$  and  $u$  as shown in Table 1.

When the samples are cooled through the transition in a magnetic field, the conductivity is anisotropic and depends on the orientation of both the sample and the magnetic field (Fig. 13). The fields of ca. 9000 oersteds used were more

14) R. P. Teele and S. Schuhmann, J. Research Nat. Bur. Standards 22, 431 (1939).

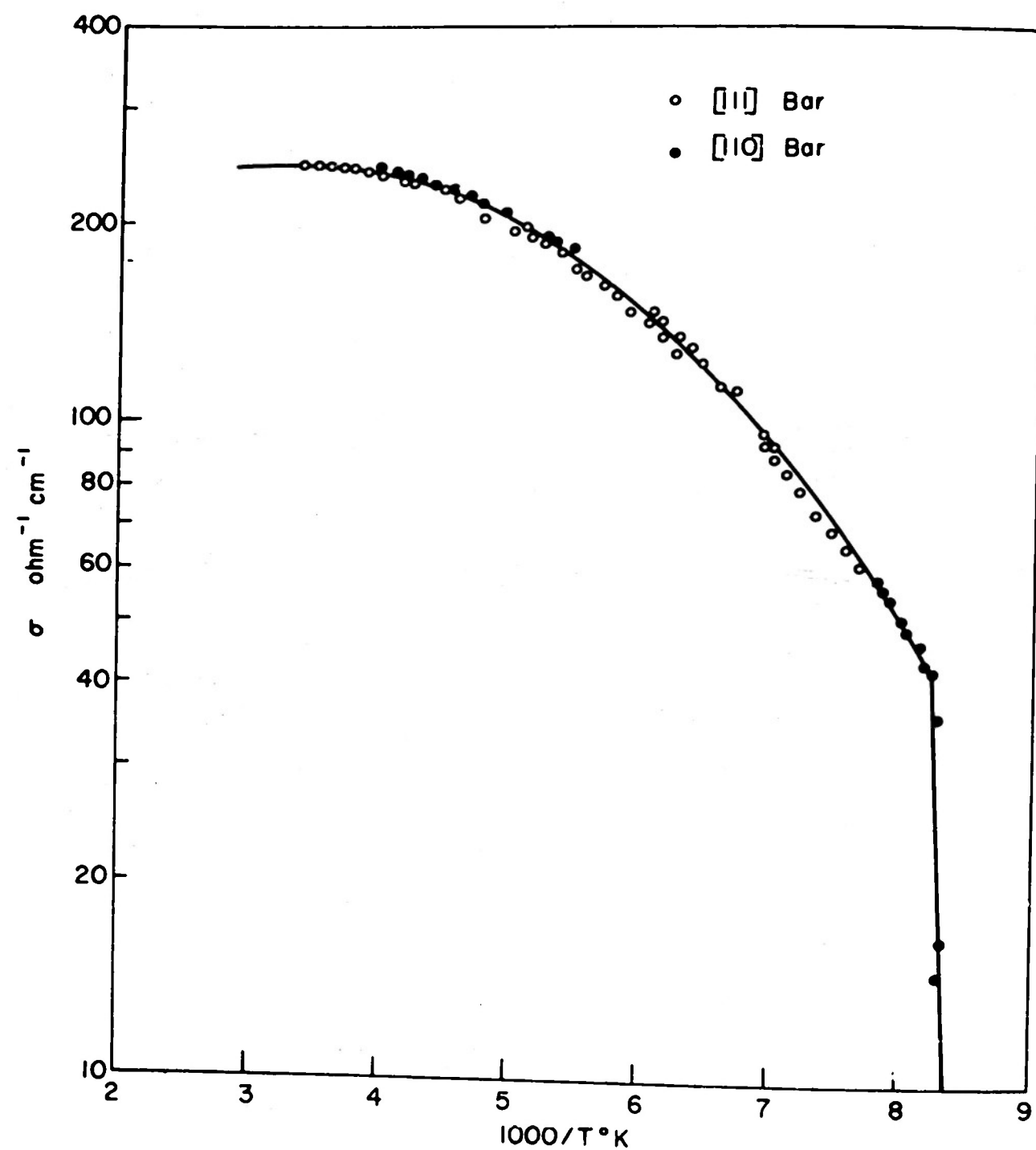


Fig. 10. Conductivity between room temperature and the transition.

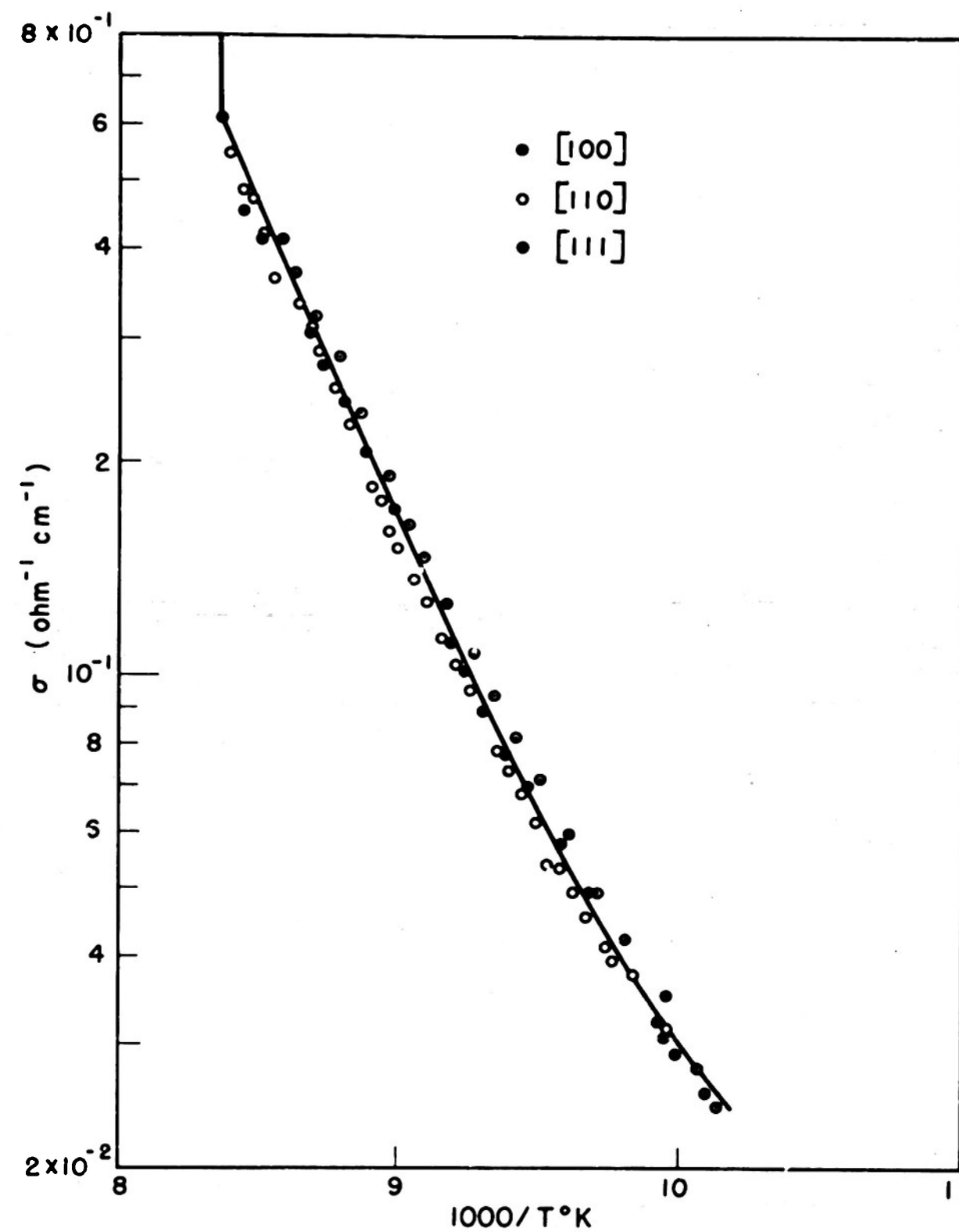


Fig. 11. Conductivity below the transition after cooling in zero magnetic field.

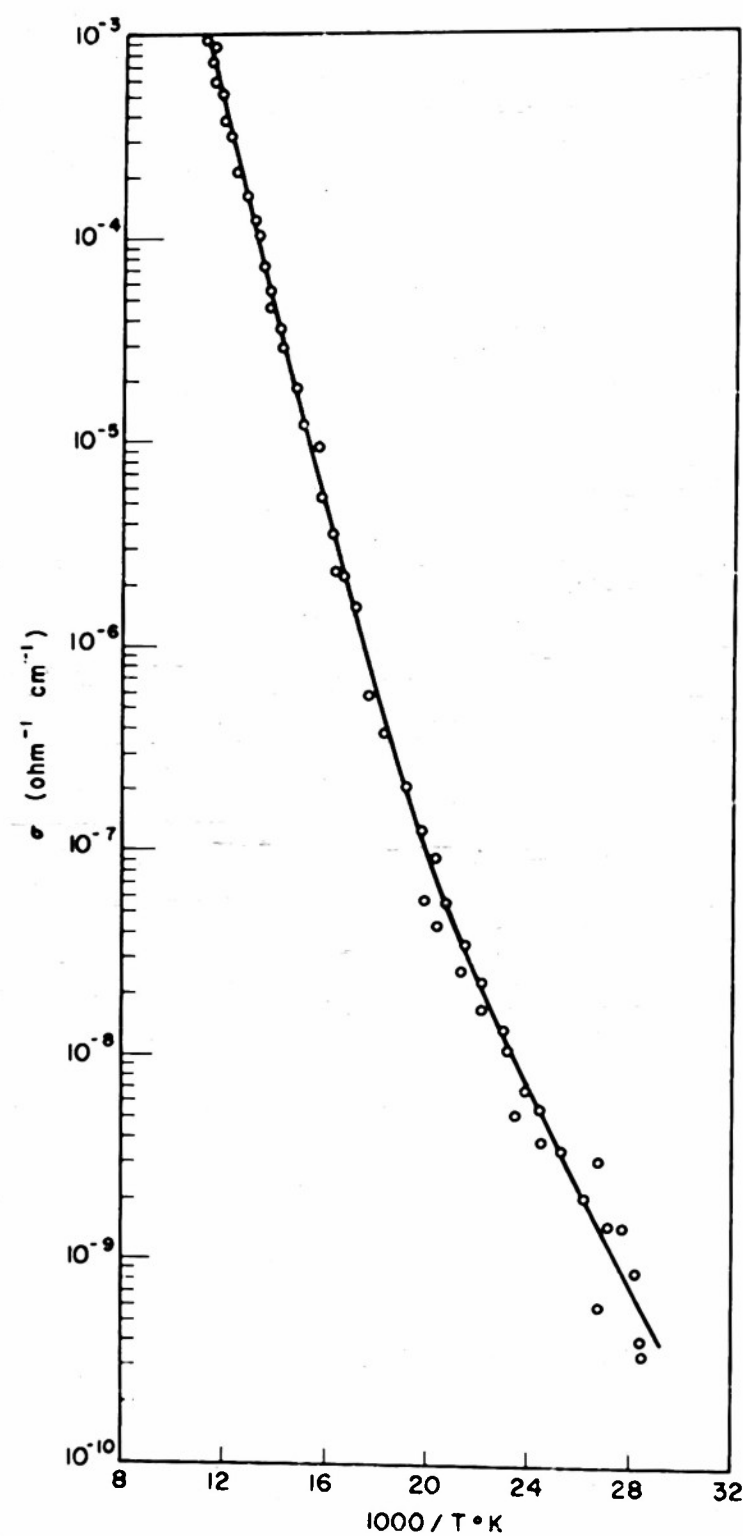


Fig. 12. Conductivity of the  $[111]$  bar from  $35^{\circ}\text{K}$  to the transition after cooling in zero magnetic field.

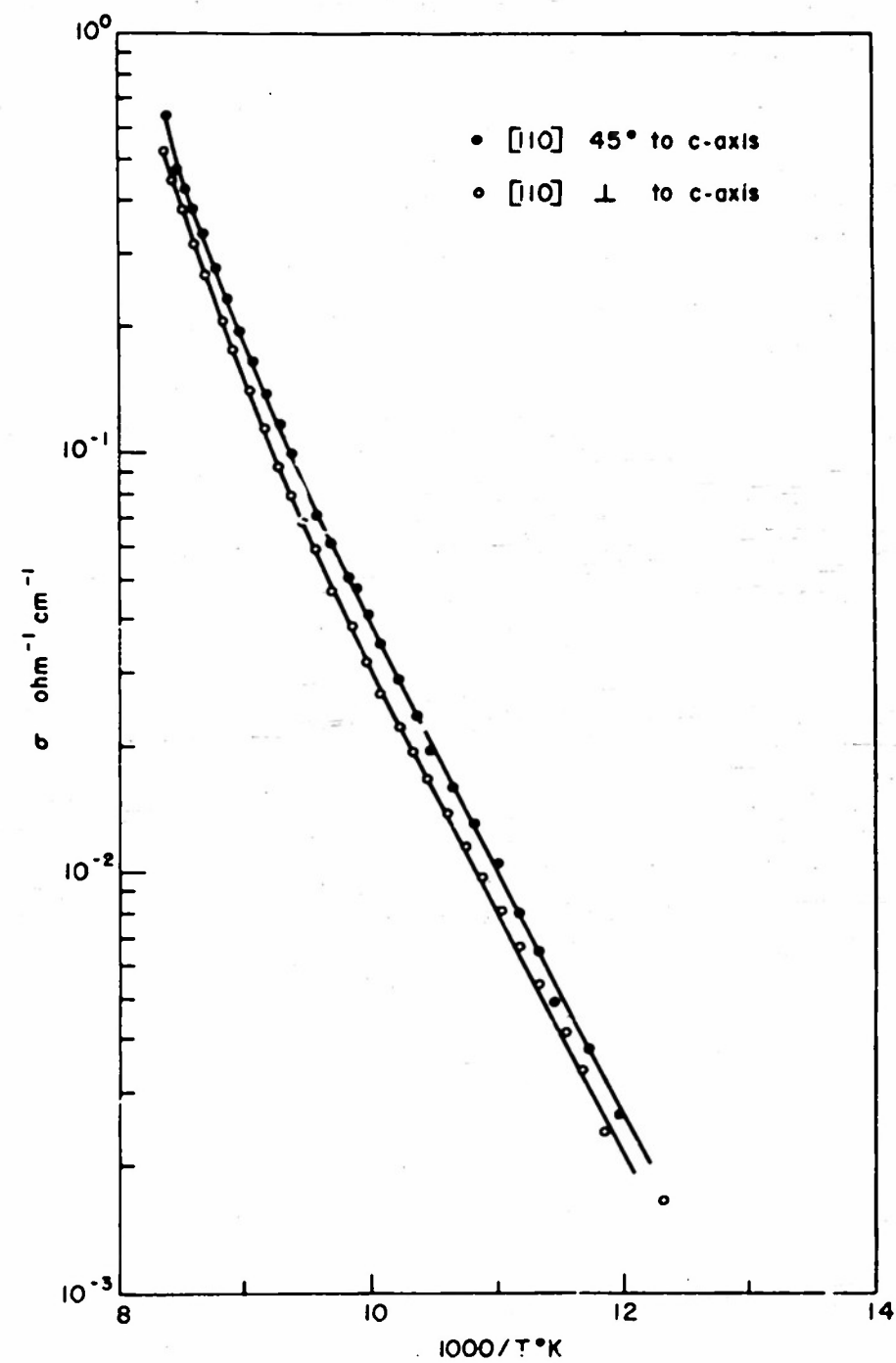


Fig. 13. Conductivity of  $[110]$  sample after cooling in two differently oriented magnetic fields.

Table 1. Conductivity of magnetite below the transition.

Temperature	A (ohm <sup>-1</sup> cm <sup>-1</sup> )	u (ev)
78 to 90°K	8200	0.11
56 to 77°	1400	0.09
40 to 52°	1.5	0.06

than sufficient to saturate the samples above the transition. The anisotropy increases rapidly from the transition to approximately 95°K, and then remains practically constant at lower temperatures. This anisotropy is quite large, the ratio of maximum to minimum conductivity being as large as 1.88. Table 2 gives the ratios of the conductivities for a number of combinations of sample orientation and magnetic field direction.

Table 2. Ratios of conductivities of magnetite in different directions below the transition

T	$\frac{\sigma[100] \parallel H}{\sigma[100] \perp H}$	$\frac{\sigma[100] \parallel H}{\sigma[110] \perp H}$	$\frac{\sigma[100] \parallel H}{\sigma[110] 45^\circ H}$	$\frac{\sigma[110] 45^\circ H}{\sigma[110] \perp H}$	$\frac{\sigma[100] \parallel H}{\sigma[111]}$
117.6°K	1.44	1.40	1.25	1.12	-
111.1	1.63	1.51	1.21	1.25	-
105.3	1.79	1.59	1.27	1.25	-
100.0	1.87	1.59	1.24	1.28	-
95.2	1.88	1.61	1.25	1.28	1.56
90.9	-	1.61	1.27	1.27	-
87.0	-	1.60	1.26	1.27	-
83.3	-	1.60	1.26	1.26	-

The observed anisotropy in the conductivity agrees well with that which can be predicted from Verwey's model of the low temperature structure of

magnetite. Although the exchange of electrons between ferrous and ferric ions has become much more difficult below the transition, it is still the dominant mechanism of conduction. In the ordered structure this will lead to an anisotropy since ferrous and ferric ions occupy adjacent sites in only four of the cubic [110] directions. Although the ordered structure has orthorhombic symmetry, its conductivity anisotropy corresponds to tetragonal symmetry (neglecting the small departure of the b/a axial ratio from unity). The conductivity of a tetragonal crystal in an arbitrary direction is given by

$$\sigma = \sigma_{11} \sin^2 \theta + \sigma_{33} \cos^2 \theta \quad (3)$$

where  $\theta$  is the angle between the direction and the c axis,  $\sigma_{33}$  the conductivity along the c axis, and  $\sigma_{11}$  the conductivity normal to the c axis. It can be seen easily from the ordered structure that the ratio  $\sigma_{33}/\sigma_{11} = 2$ . Thus we can write the conductivity below the transition as

$$\sigma = B(1 + \cos^2 \theta) \quad (4)$$

In case the order is not perfect, we would expect the conductivity to contain, in addition, an isotropic term

$$\sigma = A + B(1 + \cos^2 \theta) \quad (5)$$

The quantity  $B/(A + B)$  should be a measure of the amount of order. The values of A, B, and  $B/(A + B)$  derived from our conductivity data for a number of temperatures are given in Table 3.

Table 3. Anisotropy of conductivity below the transition.

T	A	B	B(A + B)
117.6°K	0.2660	0.1270	0.324
111.1	0.0718	0.0741	0.508
105.3	0.0202	0.0396	0.662
100.0	0.0079	0.0194	0.711
95.2	0.0026	0.01155	0.816

This table shows that with decreasing temperature the order increases, as one would expect, since the ordering process involves an activation energy.

### MAGNETIC ANISOTROPY

The magnetic anisotropy energy is the difference between the energy required to magnetize a sample in an arbitrary direction and in the direction of easy magnetization. The angular dependence of this anisotropy energy is determined by the symmetry of the crystal. In the ordered structure of magnetite a determination of the angular dependence of the anisotropy energy is particularly important since the actual deformation of the crystal structure at the transition is very small and therefore difficult to determine directly, while the anisotropy energy below the transition is very large. Consequently, the determination of the anisotropy energy provides a sensitive method for checking the crystal symmetry.

The method of calculating the dependence of the anisotropy energy on orientation for any type of crystal symmetry is well known. The anisotropy energy is expanded as a power series in the direction cosines relative to the crystallographic axes, only those terms consistent with the symmetry being retained. The existence of a plane of symmetry normal to a crystallographic axis requires the direction cosine relative to that axis to appear only in even powers. Since the ordered structure of magnetite belongs to the orthorhombic holohedral crystal class, it has three such symmetry planes (one normal to each axis). The remaining symmetry elements of this crystal class, i.e., the three two-fold axes and the center of symmetry, can be compounded from appropriate sequences of reflections in the three symmetry planes and therefore do not impose any additional restrictions on the form of the anisotropy energy. Thus we have

$$E_a = K_1 a_1^2 + K_2 a_2^2 + K_{11} a_1^4 + K_{12} a_1^2 a_2^2 + K_{22} a_2^4, \quad (6)$$

where the K's are the anisotropy constants, and the a's the direction cosines relative to the crystallographic axes. The identity  $a_1^2 + a_2^2 + a_3^2 = 1$  has been used to eliminate all the terms containing  $a_3$ . For magnetite below the transition, the c axis is the easy direction and one of the a and b axes is much harder than the other. Since this difficult axis could not be experimentally identified with one of the crystallographic axes, the b axis was arbitrary chosen as the difficult one. This choice may be inconsistent with the assignment of the true crystallographic axes but, if this should prove to be the case, only the subscripts 1 and 2 of the anisotropy constants would have to be interchanged.

The anisotropy constants were computed from the areas between the magnetization curves in different crystallographic directions. Because of the high fields needed to saturate magnetite below the transition, it was necessary to obtain the magnetization curves in fields as high as 15,000 oersteds. Since the pendulum magnetometer is, at present, limited to fields of less than 5000 oersteds, the quasistatic B-H loop tracer constructed in this laboratory<sup>15)</sup> was modified to trace the magnetization curves of samples mounted in the gap of the large electromagnet. The sample was mounted at the center of a fixed coil. The contribution of the field itself to the flux linking this coil was eliminated by mounting a second coil in the gap, some distance from the sample (Fig. 14). The two coils were connected in opposition and were adjusted to give as nearly as possible zero output with no sample in position. The voltage of these two coils was integrated and applied to one axis of a recorder. The second axis was driven by the output of a rotating coil gaussmeter, also mounted in the magnet gap. The curves obtained on the recorder are only proportional (not equal) to the magnetization, because of the flux leakage through

15) D. J. Epstein and S. Frackiewicz, Progress Rep. XI, May, 1952, p. 55.



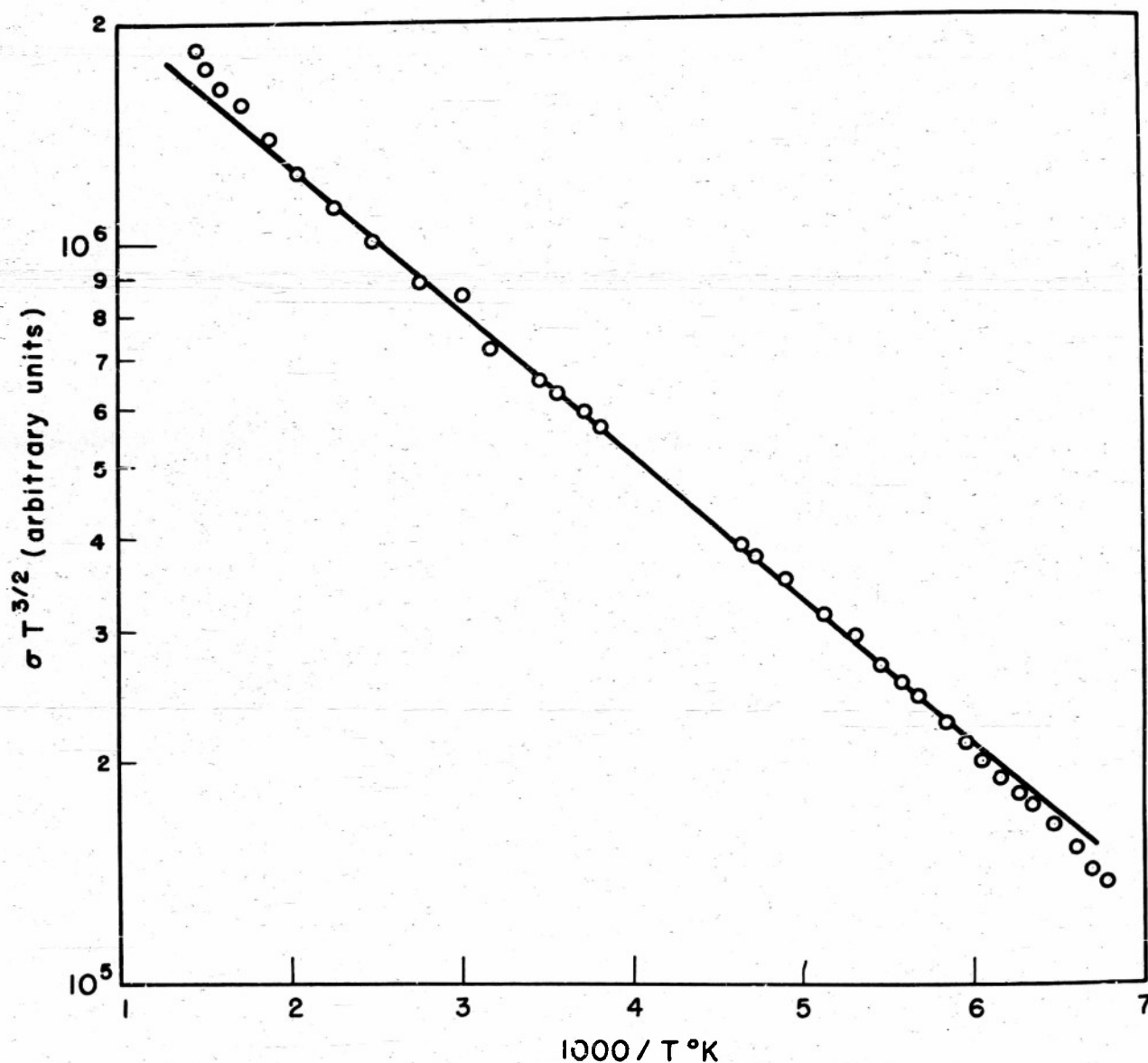


Fig. 14. Empirical relation for the conductivity above transition.

the small air gap between the sample and the coil. Since the saturation magnetization of magnetite at room temperature has been measured by a number of investigators, this was used to calibrate the scale. The sample used for these measurements was an oblate spheroid cut from a (110) plane slice of a synthetic crystal of magnetite. It was shaped by a method developed in this laboratory so that it was a much better approximation to an oblate spheroid than the (100) sample. Its axes were 3.84 and 0.97 mm, respectively, and the demagnetizing factor calculated from these dimensions was  $1.82 \pm .08$ , as compared to 1.75 computed from the [111] magnetization curve at room temperature.

Room temperature magnetization curves were measured for several reasons: the saturation magnetization at room temperature ( $477 \text{ cgs units/cc}^{2,5}$ ) was used to fix the scale of the magnetization; these curves provided a check on the demagnetizing factor calculated from the dimension of the sample; and, finally, a comparison of the anisotropy constant at room temperature with the values obtained by other methods provided an experimental check on the accuracy and reliability of the equipment. For cubic holohedral crystals, the anisotropy energy can be written as

$$E_a = K_1 (a_1^2 a_2^2 + a_2^2 a_3^2 + a_3^2 a_1^2) + K_2 a_1^2 a_2^2 a_3^2. \quad (7)$$

The value of  $K_1$  at room temperature was  $-1.12 \pm 0.05 \times 10^5 \text{ ergs/cc}$ , as determined from the areas between the [100] and [110] as well as between the [100] and [111] curves. This is in good agreement with the value of -1.12 for  $K_1$  from microwave resonance measurements<sup>1)</sup> and -1.22 from torque magnetometer measurements.<sup>13)</sup>  $K_2$  is zero, within the limits of experimental error.

The low temperature curves were obtained by immersing the sample and the surrounding coil in liquid air. The sample reached equilibrium very quickly at a temperature of ca.  $-188^\circ\text{C}$ . The saturation magnetization of magnetite

at this temperature was 508 cgs units/cc, in excellent agreement with the value of 510 at  $-195^{\circ}$  obtained by Domenicali.<sup>2)</sup> Magnetization curves were obtained in the cubic [100], [110], and [111] directions and also  $15^{\circ}$ ,  $30^{\circ}$ ,  $45^{\circ}$  and  $75^{\circ}$  to [100] after cooling with either a parallel or a perpendicular magnetic field of ca. 10,000 oersteds. Curves were also obtained in the cubic [100] and [110] directions after cooling in zero field.

The twinning that occurs in magnetite when it is cooled through the transition introduces a number of complications. A magnetic field applied to the sample as it is cooled will align the c axis along the cube edge nearest the applied field. Since the anisotropy energy is considerably lower along the a axis than along b, the a axis will tend to lie closer to the external field.<sup>16)</sup> These two conditions are sufficient to remove the twinning only in certain orientations. In some cases, particularly when the applied field makes nearly equal angles with two or three cube edges, there is uncertainty about the relative volumes of the sample which will assume each of the possible orientations. A much more serious difficulty connected with this twinning is the interactions that occur between the different regions of the sample. Thus, in many cases, a twinned sample cannot be treated by a simple superposition of the various orientations which it contains. These interactions are discussed below in detail.

The anisotropy constants were calculated by trial and error from the areas between the magnetization curves. Due to the uncertainties introduced by the possible twinning and the interactions between the different regions of the sample, a simple fitting of the measured areas between the various magnetization curves did not appear to be a sufficient check on the values of the

16) H. J. Williams, R. M. Bozorth and M. Goertz, "Mechanism of the Transition in Magnetite at Low Temperatures," Phys. Rev., in press.

Table 4. Observed and computed areas between the orthorhombic magnetization curves.

Cubic direction	Direction of cooling field	Direction cosines re orthorhombic axes	Assumed twinning	Area, ergs/cc $\times 10^{-5}$	
				calc.	obs.
$15^{\circ}$ to [001]	parallel	(1) $a_1 = .259$ (2) $a_1 = .000$ $a_2 = .000$ $a_2 = .259$	$1/2$ (1); $1/2$ (2)	0.46	1.14
$30^{\circ}$ to [001]	parallel	$a_1 = .500$ $a_2 = .000$	none	1.14	1.27
$45^{\circ}$ to [001]	parallel	$a_1 = .707$ $a_2 = .000$	none	2.55	1.35
[111]	normal	$a_1 = .816$ $a_2 = .000$	none	3.65	4.01
$75^{\circ}$ to [001]	normal	$a_1 = .966$ $a_2 = .000$	none	5.65	5.88
[110]	normal	(1) $a_1 = 1.000$ (2) $a_1 = .000$ $a_2 = .000$ $a_2 = 1.000$	$1/2$ (1); $1/2$ (2)	12.70	*
[110]	parallel	$a_1 = .500$ $a_2 = .500$	c axis twinning	4.84	4.05
$75^{\circ}$ to [001]	parallel	$a_1 = .666$ $a_2 = .300$	none	3.62	1.89
$45^{\circ}$ to [001]	normal	$a_1 = .854$ $a_2 = .146$	none	4.48	5.92
$30^{\circ}$ to [001]	normal	(1) $a_1 = .863$ (2) $a_1 = .342$ $a_2 = .342$ $a_2 = .863$	$1/2$ (1); $1/2$ (2)	10.24	8.19
$15^{\circ}$ to [001]	normal	(1) $a_1 = .813$ (2) $a_1 = .552$ $a_2 = .552$ $a_2 = .813$	$1/2$ (1); $1/2$ (2)	12.20	11.76
[001]	normal	(1) $a_1 = .707$ (2) $a_1 = .707$ $a_2 = .707$ $a_2 = .707$	$1/2$ (1); $1/2$ (2)	12.85	12.52

\* Not observed because of axis-switching.

anisotropy constants. The constants obtained from these areas were therefore used to compute the magnetization curves for the cubic [100] and [111] directions after cooling in a perpendicular field. The constants were then adjusted to improve the fit between the computed and the experimental curves. The values of the constants finally obtained were:  $K_1 = 4.0$ ,  $K_2 = 9.0$ ,  $K_{11} = 2.2$ ,  $K_{12} = 13.0$ ,  $K_{22} = 10.2 \times 10^5$  ergs/cc. The observed and calculated areas are compared in Table 4, which also shows the orientations of the orthorhombic axes used in the computations. The calculated and experimental curves for the cubic [100] and [111] directions are shown in Figs. 15 and 16. The anisotropy energy is plotted as a function of crystallographic orientation in Fig. 17.

Williams and Bozorth<sup>13,16)</sup> have measured torque curves on samples of natural magnetite at liquid nitrogen temperature, i. e., at about  $-195^\circ\text{C}$ . When their results are expressed in terms of our constants, as shown in Table 5, the agreement between the two sets of constants is relatively good, considering the differences in the temperature and the crystals used. Generally, the natural crystals are not exactly stoichiometric and consequently would not have as perfect an ordered structure as the synthetic crystals. The amount of order increases rapidly as a crystal is cooled below the transition. Thus the  $7^\circ$  difference in temperature between the two sets of measurements partially compensates

Table 5. Anisotropy constants of magnetite at low temperature.

Constants ergs/cc $\times 10^{-5}$	Method	
	Magnetization curves	Torque curves
$K_1$	4.0	2.8
$K_2$	9.0	7.5
$K_{11}$	2.2	2.2
$K_{12}$	13.0	12.4
$K_{22}$	10.2	7.4

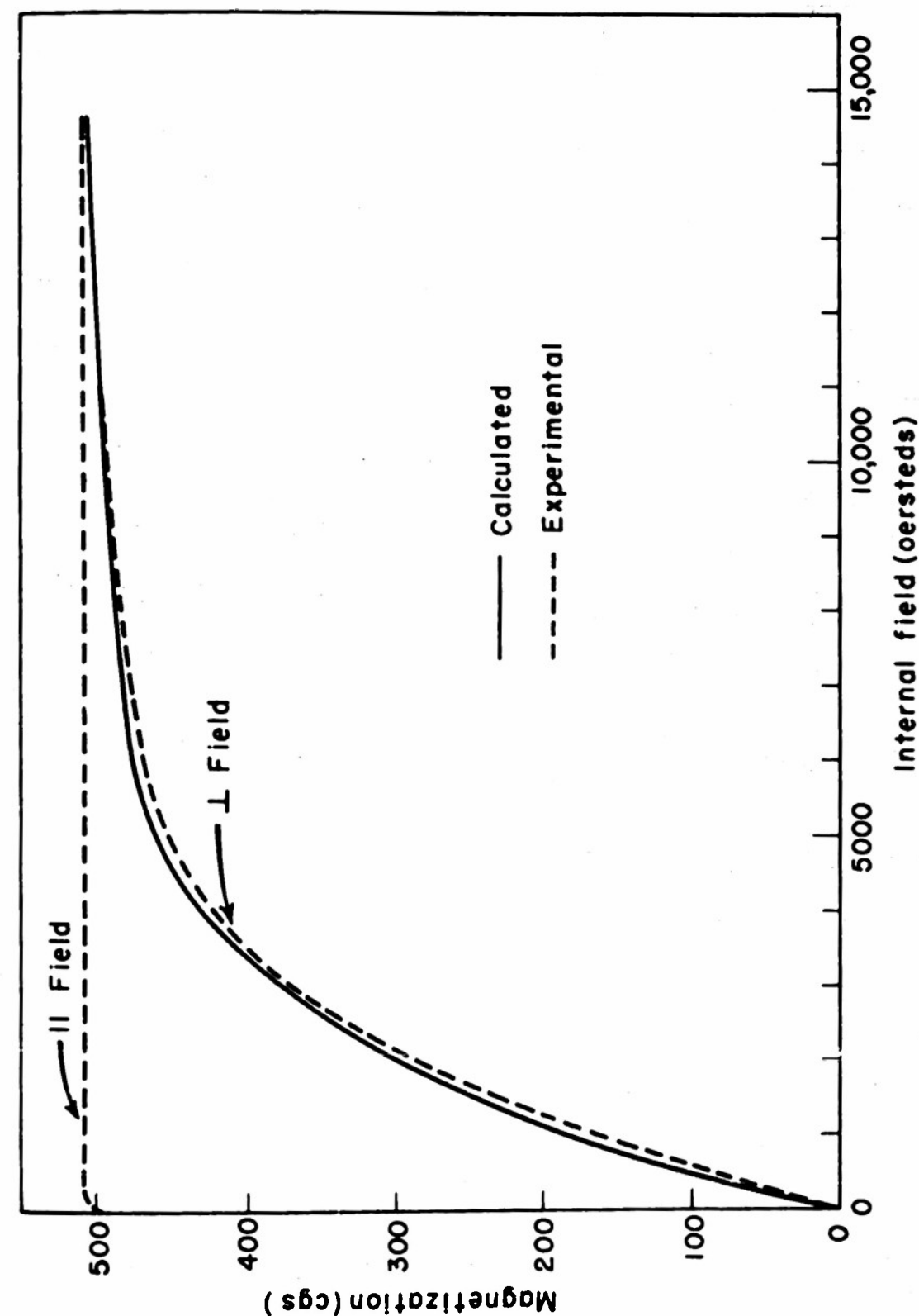


Fig. 15. Magnetization curves at  $85^\circ\text{K}$  in the [100] direction after cooling with a field of 10,000 oersteds at  $0^\circ$  and  $90^\circ$  to [100].

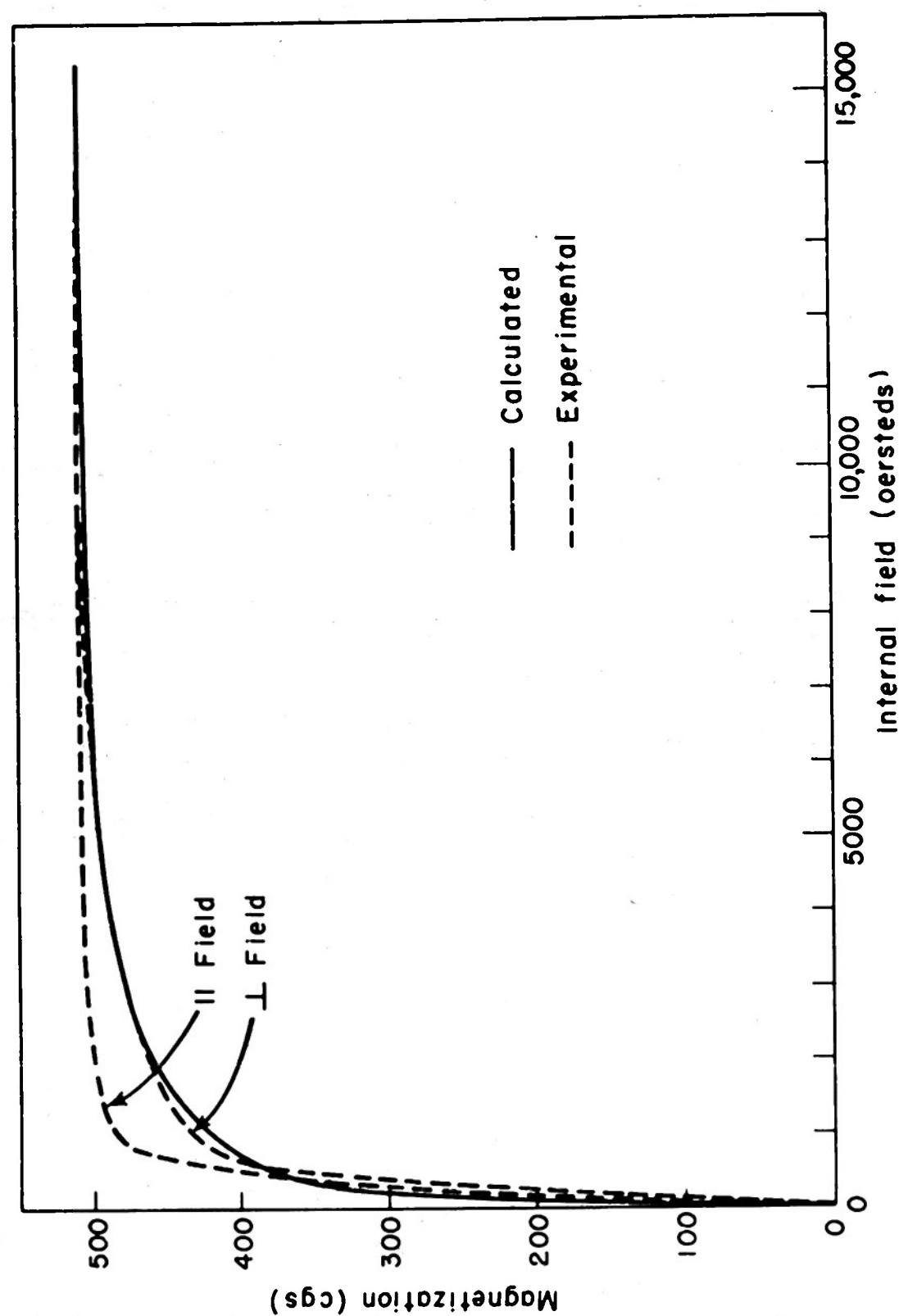


Fig. 16. Magnetization curves at 85°K in the  $[111]$  direction after cooling with a field of 10,000 oersteds at  $0^\circ$  and  $90^\circ$  to  $[111]$ .

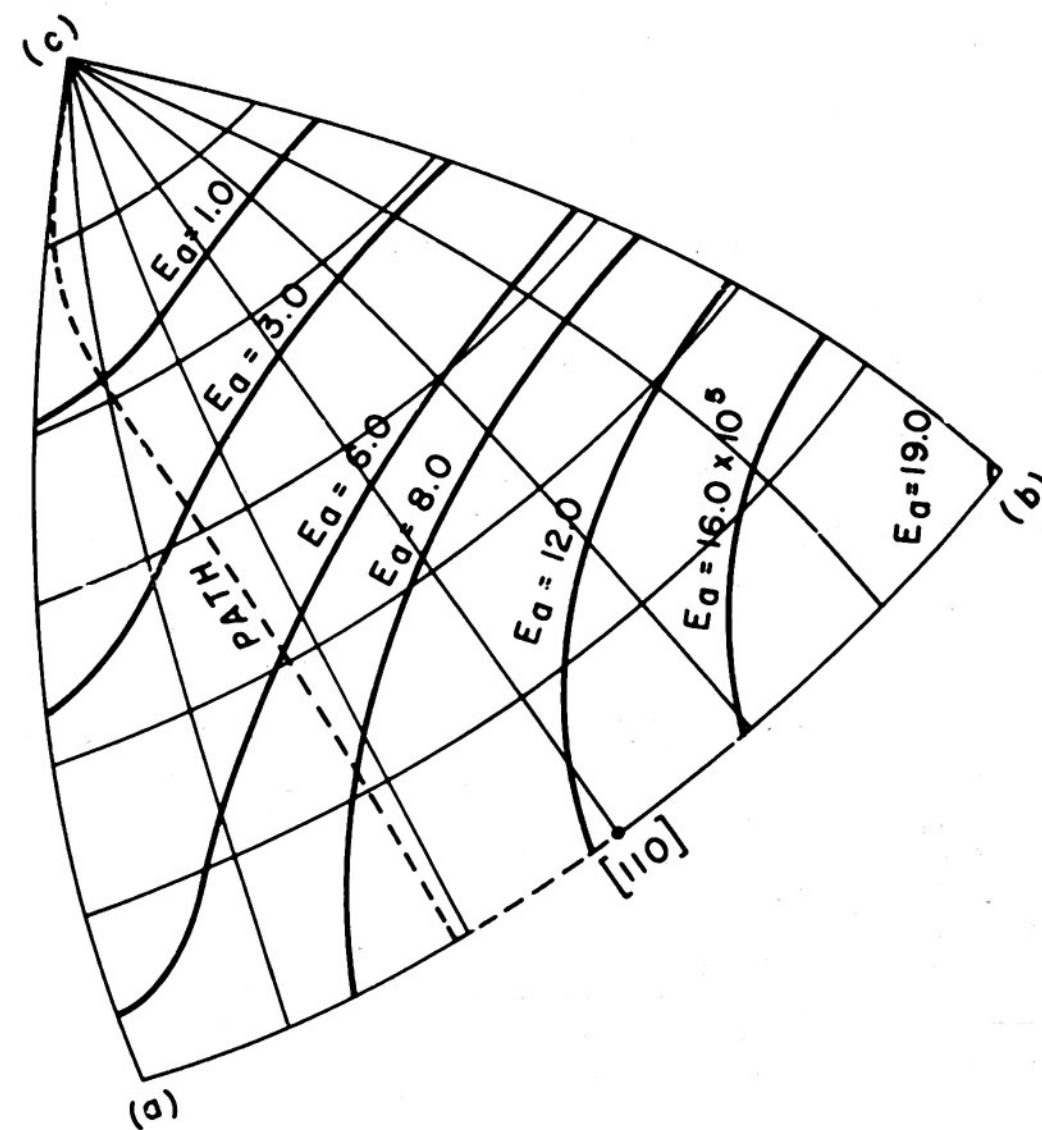


Fig. 17. Anisotropy energy of magnetite, showing the path followed by the magnetization when a field is applied in the orthorhombic  $[110]$  direction. The projections of the orthorhombic a, b, and c axes are at the corners (a), (b), and (c).

for the inherent difference in the crystals. The deviations in all constants are in the same direction. Their effect on the magnetization and torque curves is cumulative; obviously there is a real difference between the natural and the synthetic crystals.

#### INTERACTIONS BETWEEN THE REGIONS OF A TWINNED CRYSTAL

When a sample of magnetite is cooled through the transition in such a way that twinning occurs, i. e., the orthorhombic axes do not have the same orientation throughout the sample, we have a very complicated problem to deal with. The simplest assumption that can be made is that the regions of the sample in which the axes are oriented differently act completely independently of each other. Thus the behavior of the whole sample would be a simple superposition of the behavior of the individual regions. Such a simplified picture ignores the interactions between the different regions, which could arise from a number of sources: the magnetizations in neighboring regions exert torques on each other which would affect the motions under an external field; each region would be strained owing to the distortions experienced by its neighbors; and free poles on the boundaries between the regions could cause discontinuities in the internal field. The effects due to the last two causes could be very complex, and lacking the information needed to even estimate them, we can only assume that they do not greatly alter the magnetization curves.

The effect of torques exerted by the magnetization in one region on that in neighboring regions is particularly large in two of the experimental magnetization curves: the cubic [100] direction cooled in zero field, and the cubic [111] direction cooled in a parallel field. When a sample is cooled through the transition in demagnetized state, the cubic [100] direction will become the

orthorhombic [001] in 1/3 of the sample; the orthorhombic [110] in 1/3; and the orthorhombic [110] in 1/3, since the orthorhombic a and b axes develop along face diagonals of the cubic unit cell. The magnetization curves in the orthorhombic [110] and [110] directions will be identical. The orthorhombic [110] curve can be obtained by cooling with a field normal to the cubic [100] direction, and the [001] curve with a parallel field. Since the c axis (001) is the easy direction, if there were no interaction, the magnetization curve for the cubic [100] direction, after cooling in zero field, should be given by

$$H_0 = H_L ; I_0 = I_H/3 + 2I_L/3 \quad (8)$$

All these quantities can be obtained from the curves in Fig. 15. The curve calculated from this equation is compared in Fig. 18 with the experimental curve. The discrepancy is due to the interaction between the different regions, which causes an additional torque to affect the magnetization. In part of the sample, there is magnetization  $I_s$  parallel to the field and in the remainder of the sample, a magnetization  $I_s$  at an angle  $\theta$  to the field. The magnetization parallel to the field will exert a torque on the remainder of the magnetization. The energy arising from this torque will be of the form  $I_s^2 \cos \theta$ . Thus the energy of a region whose c axis is perpendicular to the applied field will be

$$E_T = E_a - HI_s \cos \theta - CI_s^2 \cos \theta \quad (9)$$

where  $E_a$  is the anisotropy energy,  $H$  the internal field,  $I_s$  the saturation magnetization, and  $C$  an empirical constant. To find the equilibrium position of the magnetization, we set  $dE_T/d\theta = 0$  and obtain

$$H - CI_s = -dE_a/d\theta/I_s \sin \theta \quad (10)$$

The corresponding equation for a sample containing only regions with their c axes normal to the applied field is the same except that the term  $-CI_s$  is not present. Therefore, the magnetization curve for the cubic [100] direction

cooled in zero field will be given by the equation

$$H_0 = H_{\perp} - CI_s ; I_0 = I_{\parallel}/3 + 2I_{\perp}/3 \quad (11)$$

The fit between this equation with  $C = 1$ , and the experimental curve is quite satisfactory (cf. Fig. 18). The discrepancy in fields below 800 oersteds is due to strains induced in the sample as it cooled through the transition, and to the effects of the magnetostriction. A comparison of this curve with that for the cubic [100] direction cooled in a parallel field indicates that these effects are much larger here, as we would expect.

This case is one in which the interaction has a very large effect on the magnetization curve for two reasons: the interaction torque is large because the angle between the magnetizations is large; and this torque acts in the same direction as the torque due to the applied field. Another case in which these conditions are present is that of the cubic [111] direction cooled in a parallel field. In this case, the  $c$  axis will be distributed over all three cube edges with the  $a$  and  $b$  axes so oriented that the cooling field lies in an  $a$ - $c$  plane throughout the sample. The interaction is more complicated here because each magnetization will be subject to two interaction torques and, in addition, the angle between two magnetizations is not the same as the angle between each one and the applied field. We can see the effect of the interaction directly by comparing the cubic [111] curves after cooling in different fields. After cooling in a perpendicular field, the cubic (110) plane will transform into the  $a$ - $c$  plane of the orthorhombic crystal, with no multiple orientation. Thus the difference in the two cubic [111] curves (Fig. 16) is due to the interaction occurring after cooling in a parallel field. In most of the other cases we have observed, the effects of the interactions will be much smaller.

These interactions probably account for the failure of the anisotropy

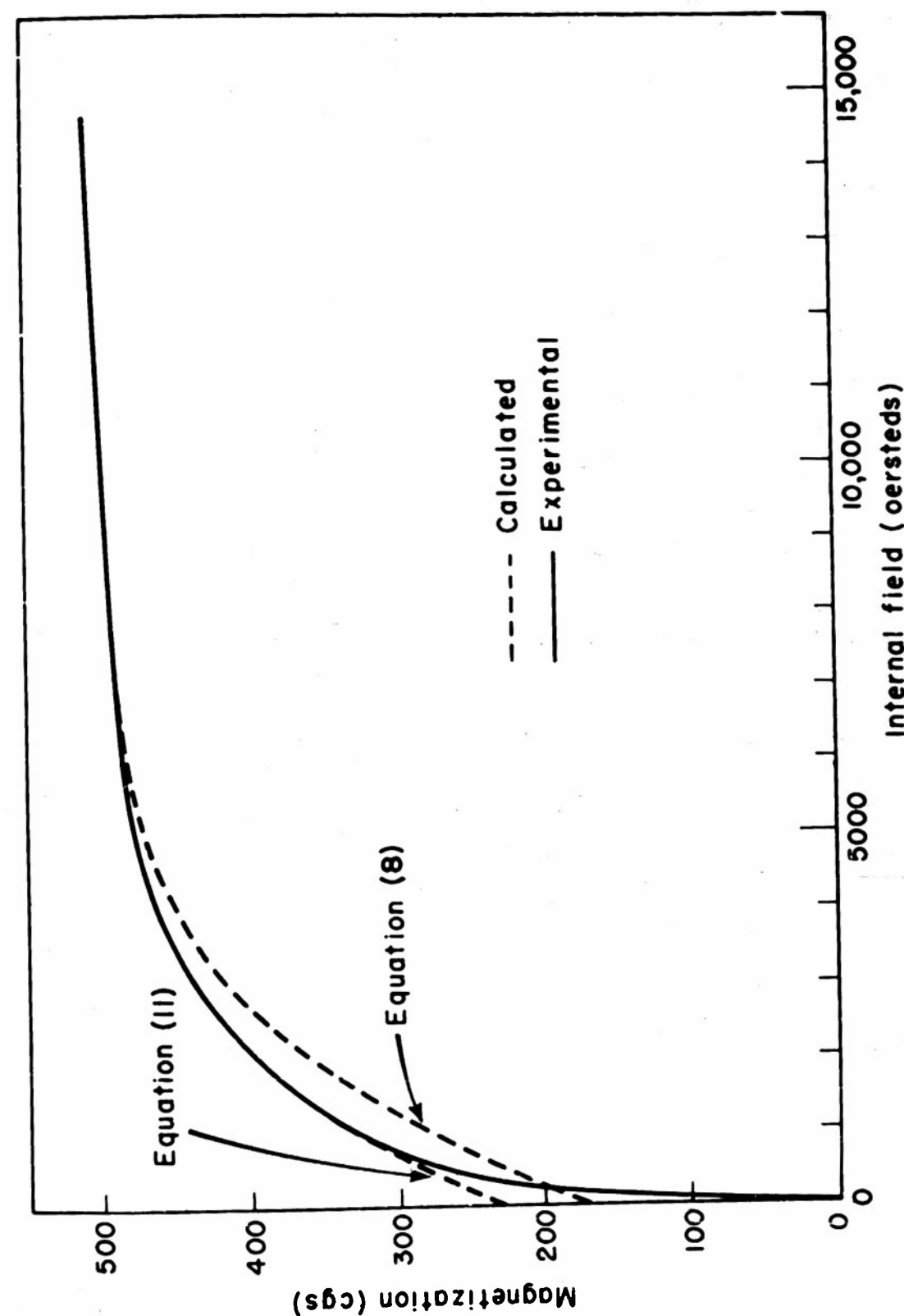


Fig. 18. Magnetization curve at 85°K in the [100] direction after cooling in zero field.



constants obtained by static methods, to explain the microwave resonances observed by Bickford.<sup>1)</sup> The twinning that occurs at the transition accounts qualitatively for the multiple resonances observed, except in the case of the cubic (100) plane. Some of the resonances in this plane may be due to lack of magnetic saturation in the sample. When the observed anisotropy constants are used to calculate the positions of the resonance peaks, these calculated values do not agree with those observed. Interactions of the type described above produce torques which would affect the precession of the magnetization and hence the position of the resonance. It will be necessary to perform these experiments again under conditions such that no twinning occurs in order to determine whether the static anisotropy constants will account for the experimental results.

#### SUMMARY AND CONCLUSIONS

The orthorhombic structure of magnetite below the transition is confirmed by a wide variety of experimental evidence. Direct determination of the unit cell size, both by X rays<sup>10)</sup> and strain-gauge measurements,<sup>11)</sup> show that the orthorhombic axes are oriented so that the c axis lies along one of the original cube edges and the a and b axes along the perpendicular cubic face-diagonal directions. The magnetic anisotropy energy gives perhaps even more convincing evidence since it is so large that there can be no doubt about its form, whereas the changes in the unit cell itself are very small. The anisotropy of the conductivity agrees with that to be expected from Verwey's ordered structure.

In addition to accounting for the anisotropic properties below the transition, Verwey's model explains the influence of a magnetic field, applied during cooling on the properties of the crystal below the transition. The axis-switching effect was not predicted from this model, but the model does provide an

explanation for it. While it is true that the ordering has not been directly observed, e.g., superlattice lines have not yet been found in X-ray or neutron diffraction experiments, it accounts so completely and quantitatively for the behavior of magnetite at and below its low-temperature transition that there can be little doubt of the correctness of Verwey's hypothesis.

The twinning which occurs at the transition greatly complicates the magnetic behavior at lower temperatures because the different regions of a twinned crystal interact in a complex way with each other. These interactions are quite large in some cases and probably account for the failure of the static anisotropy constants to explain the microwave resonance data.

One remaining problem of major interest concerning the low-temperature region of magnetite is a detailed interpretation of the conductivity data. The increase in conductivity anisotropy with decreasing temperature (Table 3) appears to be directly related to the increase in long-range order. A greatly over-simplified band model, which exhibits a discontinuity in the conductivity such as that in magnetite at the transition, is described in Appendix 3. Such models must necessarily be very speculative until much more experimental data become available particularly on the Hall effect and the thermoelectromotive force.

#### ACKNOWLEDGMENTS

The author is greatly indebted to Professor A. von Hippel for his guidance and encouragement during the course of this research; to B. Frankiewicz for his assistance with the B-H loop tracer measurements; to many members of this laboratory, in particular, D. J. Epstein, D. O. Smith and L. B. Smith, for the many discussions and helpful suggestions made during the course of this work. The author wishes also to thank R. P. Teele of the



National Bureau of Standards for the loan of the "thermo-free" reversing key used in the low-temperature thermocouple potentiometer. Finally, the author's thanks are due to L. R. Bickford, Jr., R. M. Bozorth, and J. M. Lavine for the privilege of seeing their results prior to publication.

#### Appendix 1.

#### DETAILS OF THE CALCULATION OF THE LOW TEMPERATURE MAGNETIZATION CURVES

The calculation of the magnetization curve in the cubic  $[111]$  direction of a sample cooled in a magnetic field normal to this direction in a  $(110)$  plane, proceeds as for a cubic crystal. Both the easy ( $c$ -axis) direction and the applied field lie in the  $a$ - $c$  plane of the orthorhombic structure and there is no twinning to complicate the problem. Since the anisotropy energy is symmetric about this plane, there will be no torque acting to move the magnetization out of the plane and its equilibrium position will be determined by the condition that the total energy

$$E_T = E_a - H I_s \cos(54^\circ 44' - \theta) \quad (12)$$

is a minimum ( $\theta$  is the angle between  $I_s$  and  $c$  axis). The anisotropy is given by

$$E_a = K_1 \sin^2 \theta + K_{11} \sin^4 \theta \quad (13)$$

Setting  $dE_T/d\theta = 0$ , we obtain

$$H = (K_1 \sin 2\theta + 2K_{11} \sin^2 \theta \sin 2\theta) / I_s \sin(54^\circ 44' - \theta) \quad (14)$$

and we have

$$I = I_s \cos(54^\circ 44' - \theta) \quad (15)$$

From these parametric equations, the magnetization curve can be computed.

The calculation for a cubic  $[100]$  direction cooled with a field along a perpendicular  $[110]$  is much more complicated. We will neglect the interactions between the different regions, since the experimental curves (Fig. 15)

indicate that in this case they do not significantly affect the magnetization curve. This curve will be that for the orthorhombic  $[110]$  direction. The anisotropy energy is not symmetric about the orthorhombic  $(110)$  plane, and consequently there will be a torque acting to turn the magnetization out of this plane. To find the path followed by the magnetization, we use the spherical co-ordinates indicated in Fig. 19 and express the anisotropy energy in terms of the angles  $\theta$  and  $\phi$ . Since the field exerts no torque in the direction of  $\phi$ , the path will be determined by the condition

$$\partial E_a / \partial \phi = 0 \quad (16)$$

In this case, we have

$$\begin{aligned} a_1 &= \frac{1}{(2)^{1/2}} (\cos \theta + \sin \phi \sin \theta) \\ a_2 &= \frac{1}{(2)^{1/2}} (\cos \theta - \sin \phi \sin \theta) \end{aligned} \quad (17)$$

and, substituting these expressions into the anisotropy energy (Eq. 6) and differentiating, we obtain

$$\begin{aligned} &\cos \phi \left\{ \sin^3 \phi [(K_{11} + K_{12} + K_{22}) \sin^4 \theta] \right. \\ &+ \sin^2 \phi [3(K_{11} - K_{22}) \sin^3 \theta \cos \theta] \\ &+ \sin \phi [(3K_{11} - K_{12} + 3K_{22}) \sin^2 \theta \cos^2 \theta + (K_1 + K_2) \sin^2 \theta] \\ &\left. + [(K_{11} - K_{22}) \sin \theta \cos^3 \theta + (K_1 - K_2) \sin \theta \cos \theta] \right\} = 0. \end{aligned} \quad (18)$$

If  $\phi \neq 90^\circ$ , this is a cubic equation in  $\sin \phi$ . For values of the anisotropy con-

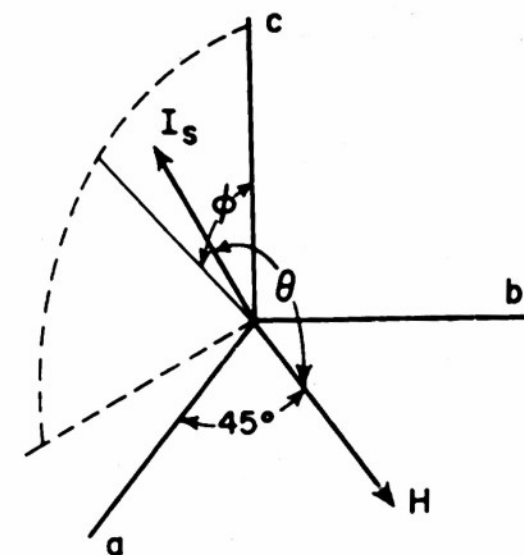


Fig. 19. Co-ordinate system for calculation of orthorhombic 110 magnetization curve.

stants in the range of those of magnetite, this equation has only one real root. We can find any number of points along the path of the magnetization by substituting various values of  $\theta$  into this equation and solving numerically for the corresponding values of  $\theta$ . The path is indicated in Fig. 17. This method is applicable for any orientation of the applied field relative to the crystallographic axes and for any type of crystal symmetry. In many cases, however, a graphical method described by Bozorth and Williams<sup>17)</sup> would be less laborious.

With the path determined, we can set up the equations for the magnetization curve. The energy is given by

$$E_T = E_a - HI_s \cos \theta \quad (19)$$

and, after differentiating, we obtain

$$H = - \partial E_a / \partial \theta / I_s \sin \theta \quad (20)$$

We then have

$$I = I_s \cos \theta \quad (21)$$

The derivative  $\partial E_a / \partial \theta$  is given by

$$\begin{aligned} \partial E_a / \partial \theta = & -1/2 (K_1 + K_2) \sin 2\theta \cos^2 \phi + (K_1 - K_2) \sin \phi \cos 2\theta \\ & -1/2 (K_{11} + K_{12} + K_{22}) \cos^2 \theta \sin 2\theta \\ & +1/2 (K_{11} + K_{12} + K_{22}) \sin^4 \phi \sin^2 \theta \sin 2\theta \\ & +1/4 (3K_{11} - K_{12} + 3K_{22}) \sin^2 \phi \sin 4\theta \\ & -3/4 (K_{11} - K_{22}) \sin \phi \cos^2 \phi \sin^2 2\theta + (K_{11} - K_{22}) \sin \phi \cos^4 \theta \\ & - (K_{11} - K_{22}) \sin^3 \phi \sin^4 \theta \end{aligned} \quad (22)$$

and must be evaluated at points along the path of the magnetization.

## Appendix 2.

### MAGNETOSTRICTION OF MAGNETITE AT ROOM TEMPERATURE

Measurements of the magnetostriction of natural crystals of magnetite,<sup>18)</sup> indicated that its behavior was very unusual in that the longitudinal saturation magnetostriction in the  $[110]$  direction was not intermediate between that for the  $[100]$  and  $[111]$  directions. The magnetostriction of the synthetic crystals of magnetite was measured using the dilatometer constructed by Domenicali.<sup>2)</sup> Changes in the length of the sample alter the separation, and hence the capacitance, of two metal plates. These changes in capacitance were measured with a beat-frequency equipment developed in this laboratory.<sup>19)</sup> With this apparatus, the minimum change in length that could be measured was  $6 \times 10^{-7}$  mm. The dilatometer was calibrated by measuring the thermal expansion of magnetite, nickel and fused quartz between  $15^\circ$  and  $30^\circ$  C.

The samples used for the magnetostriction measurements were the rectangular bars used for the conductivity measurements. The observed magnetostriction depends in a complicated way on the shape of the sample and the elastic constants.<sup>20)</sup> In iron, this correction for the "form effect" is extremely important but, since it is proportional to the square of the magnetization, it is very small in magnetite (of the order of  $10^{-7}$ ) and was ignored. The most serious drawback of the bar-shaped samples is that the demagnetizing field is not uniform. Hence, the magnetization processes are smeared out and the magnetostriction data do not provide information on the various translational and rotational processes occurring during the magnetization of the sample. Only the saturation magnetostrictions have full significance.

18) C. W. Heaps, Phys. Rev. 24, 60 (1924).

19) J. G. Jelatis, Tech. Rep. 7; J. Appl. Phys. 19, 419 (1948).

20) R. Becker and W. Döring, "Ferromagnetismus," Springer, Berlin, 1939, p.305.

17) R. M. Bozorth and H. J. Williams, Phys. Rev. 59, 827 (1941).

The longitudinal magnetostriction was measured in the three crystallographic directions [100], [110], [111]. The transverse magnetostriction was measured by rotating the dilatometer 90° in the magnet gap, so that the field was applied parallel to a short dimension of the sample and the elongation measured along the length. It was apparent from the values of the longitudinal saturation magnetostrictions that the usual two-constant expression for the magnetostriction could not be made to fit the data. The experimental values were fitted to a five-constant expression<sup>21)</sup>

$$\begin{aligned} \delta l/l = & h_1(a_1^2\beta_1^2 + a_2^2\beta_2^2 + a_3^2\beta_3^2 - 1/3) \\ & + h_2(2a_1a_2\beta_1\beta_2 + 2a_2a_3\beta_2\beta_3 + 2a_3a_1\beta_3\beta_1) \\ & + h_3(s - 1/3) + h_4(a_1^4\beta_1^2 + a_2^4\beta_2^2 + a_3^4\beta_3^2 + 2s/3 - 1/3) \\ & + h_5(2a_1a_2a_3^2\beta_1\beta_2 + 2a_2a_3a_1^2\beta_2\beta_3 + 2a_3a_1a_2^2\beta_3\beta_1), \end{aligned} \quad (23)$$

where  $a$ 's are the direction cosines of the magnetization,  $\beta$ 's the direction cosines of the elongation, and  $s = a_1^2a_2^2 + a_2^2a_3^2 + a_3^2a_1^2$ . Since  $h_3$  represents the volume magnetostriction, which is very small compared to the linear effect, we may place  $h_3 = 0$ .

The experimental results were fitted by taking

$$h_1 = 547, \quad h_2 = 111, \quad h_4 = -576, \quad h_5 = 56 \times 10^{-6}$$

The calculated and observed values are compared in Table 6. The information is too scanty to permit these constants to be very precisely determined;  $h_5$ , particularly, may be in error by a factor of 2 or more, since it appears to a significant extent only in the expression for the longitudinal magnetostriction in the [111] bar.

21) R. Becker and W. Düring, op. cit., pp. 273-81.

Table 6. Comparison of calculated and observed saturation magnetostriction at 15°C.

Direction of H	Direction of $\delta l/l$	Theoretical expression	$\delta l/l \times 10^6$ calculated	$\delta l/l \times 10^6$ observed
[110]	[110]	$h_1/6 + h_2/2 + h_4/12$	98.7	101
[111]	[111]	$2h_2/3 + 2h_5/9$	86.4	88
[100]	[100]	$2h_1/3 + 2h_4/3$	-19.4	-16
[211]	[111]	$-h_2/3$	-37	-28
[001]	[110]	$-h_1/3 - h_4/3$	9.7	12
[110]	[110]	$h_1/6 - h_2/2 + h_4/12$	-12.3	-21
[010]	[100]	$-h_1/3 - h_4/3$	9.7	6.7
	ceramic*	$4h_1/15 + 2h_2/5 + 8h_4/35 + 2h_5/35$	61.9	61

### Appendix 3.

#### A BAND MODEL FOR MAGNETITE

Throughout the preceding discussion, we have assumed an ionic model for magnetite. This approach provides an explanation of the transition and of the conductivity. It yields correct information about the relative stability of the normal and inverse spinel structure for the ferrites, and similar oxides of aluminum and chromium,<sup>7, 22)</sup> and predicts on the basis of a calculation of the Madelung energy\* that the ordered structure of magnetite is slightly more

22) E. J. W. Verwey, F. de Boer and J. H. van Santen, J. Chem. Phys. 16, 1091 (1948).

\* The actual value of the calculated energy difference between the ordered and the disordered structure is ca. 1 ev per  $\text{Fe}_3\text{O}_4$ , as compared to an observed difference (from specific heat measurements) of 0.005 ev, and has little significance, since it is obtained by subtracting two relatively large numbers. Also the calculated energy of the ordered structure is based on the assumption that the ions occupy the same relative positions in both structures, which is not true; this may account for the discrepancy.

stable than the disordered one.<sup>23)</sup>

Several attempts by Miyahara<sup>24)</sup> to set up a band model for the ferromagnetic semiconductors have not been very successful. His basic assumption was that a large exchange energy between electrons in the valence band would lead to ferromagnetism because of holes, i.e., when electrons were removed from the valence band the remaining electrons would have a nonzero spin. Any theory based on this assumption must lead to a disappearance of the ferromagnetism at a sufficiently low temperature, a behavior thus far not observed in any material. Verwey claims that in the oxides of the transition metals, the highest occupied levels are those arising from metallic 3d states, while the energy levels of the oxygen lie considerably lower.<sup>25)</sup> The actual form of the 3d band of the iron ions in magnetite would be quite complicated, since the levels arising from ions in octahedral and tetrahedral interstices will not coincide. The exchange energies responsible for the magnetism will cause complicated shifts in the levels depending on the spin of the electron.

There is no obvious way of estimating these various effects. Although the whole picture is probably greatly oversimplified, we can make some tentative calculations on the following basis: the 3d levels in magnetite are supposed to be split into two bands, separated by a relatively narrow gap. We neglect the magnetic interactions in magnetite. In distributing the electrons between the two bands, we arrange that the lower band shall be filled at absolute zero, and the upper band empty. Hence we must have 128 levels/unit cell in the valence band and 112 levels/unit cell in the conduction band. To keep the calculations as simple as possible, we have assumed that these bands

23) F. de Boer, J. H. van Santen and E. J. Verwey, J. Chem. Phys. 18, 1032 (1950).

24) S. Miyahara, Phys. Rev. 55, 105 (1939); Z. Physik 113, 247 (1939); Proc. Physico-Math. Soc. Japan 24, 49 (1942); T. Hirone and S. Miyahara, *ibid.* 24, 560 (1942).

25) E. J. W. Verwey, "Semiconducting Materials," Butterworth, London, 1951, p. 151.

are parabolic. The widths were obtained by requiring that  $\int_{\text{band}} (dN/dE)dE$  equal the total number of levels in the band. At the energy at which this occurred,  $dN/dE$  was assumed to drop discontinuously to zero. This actually had no effect on the calculations, since at the highest temperature used,  $kT$  was less than one third of the width of the valence band. In the calculation of the number of carriers, we can ignore such small effects and assume that the bands are parabolic and extend to infinity.

There is still nothing in this picture to lead to the observed transition. To account for the transition, we suppose that each ferrous ion has a localized energy level, which lies in the energy gap between the two bands. Since the energy gap itself is very narrow, these localized levels must lie close to the valence band. At some temperature there will be a sufficient number of these levels occupied so that a considerable overlap will occur between neighboring wave functions. When this happens electrons can be transferred from one localized level to another. Then these levels will broaden slightly into a band, and conduction can occur in this band.

To make this idea quantitative, we must consider the distribution of the ions in the ordered structure. Surrounding a ferrous ion is the following arrangement of other ferrous ions: two at 2.97Å; four at 5.14Å; twelve at 5.93Å; four at 6.63Å; eight at 7.85Å; six at 8.39Å. The radius of the wave functions of these localized levels will be  $\kappa a_0$ , where  $\kappa$  is the dielectric constant and  $a_0$  is the Bohr radius. If we assume a dielectric constant of ca. 11, the radius of the wave function will extend approximately to the twelve neighboring ferrous ions at a distance of 5.93Å, and significant amounts of overlap will occur when a neighbor within a distance of 5.93Å is also excited. We expect the transition to occur when 1/18 of the ferrous ions are excited. Since there are  $1.354 \times 10^{22}$  ferrous ions/cc, the transition will occur when  $7.52 \times 10^{20}$

electrons/cc have been excited to localized levels.

After a number of trials, the band scheme indicated in Fig. 20 was adopted. The effective masses for electrons and holes are, respectively, 35 and 55. The widths of the valence (0.24 ev) and the conduction (0.35 ev) bands are narrow compared to the width of the 3d band in the transition metals (ca. 5 ev). Taking the top of the valence band as the zero of energy, we can immediately write

$$p = 1.96 \times 10^{18} T^{3/2} \exp(-E_f/kT)$$

$$n_c = 9.83 \times 10^{17} T^{3/2} \exp(E_f - .12/kt)$$

$$n_e = 1.35 \times 10^{22} (1 + \exp(.45 - E_f/kT))^{-1}$$

where  $p$  is the number of holes in the valence band;  $n_c$  is the number of electrons in the conduction band;  $n_e$  is the number of electrons in the localized levels. These equations for  $n_c$  and  $p$  are valid only if  $kT$  is small compared to  $E_f$  and  $E_f - 0.12$ . Obviously, these conditions will be satisfied only at very low temperatures in the present model. A convenient method of calculating  $p$  and  $n_c$  when  $kT$  is not small was worked out and used in the calculations.

This model can account qualitatively for the observed axis-switching. The transfer of electrons from ferrous to neighboring ferric ions below the transition can occur through these localized excited levels. This immediately leads us to expect practically identical activation energies for axis-switching and for the conductivity above the transition. The experimental values are 0.033 and 0.039. The band model also accounts for the maximum observed in

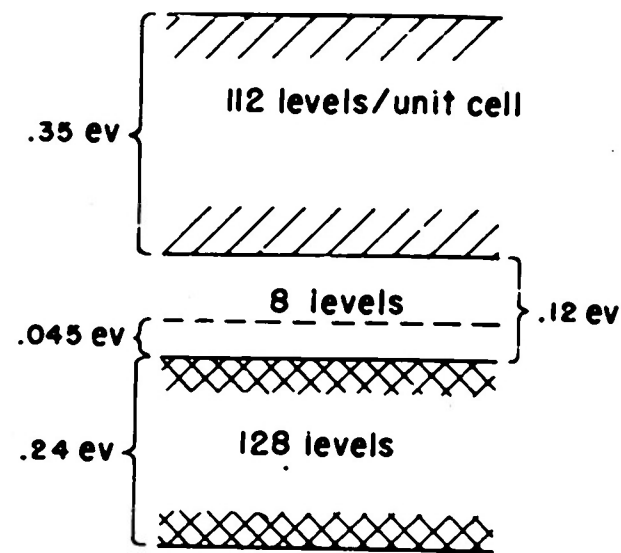


Fig. 20. Schematic diagram for the energy levels of magnetite.

the conductivity at ca. 15°C. Since the number of carriers does not increase very much with temperature, the increased scattering at higher temperatures becomes sufficient to cause the conductivity to decrease with increasing temperatures.

In this model, we have four adjustable parameters: the effective masses in the valence and conduction bands; the width of the gap; the location of the localized energy levels in the gap. There are two conditions which we can impose on this model. One is that it yield the correct transition temperature and the other, that it show the correct increase in conductivity at ca. 550°C. There are many combinations of the parameters which will satisfy these two requirements. To determine a particular model, it is necessary to include some more or less arbitrary additional conditions. In the model actually used, one of these conditions was that the Fermi level lie in the middle in the middle of the gap at 550°C. Since the model is so greatly over-simplified, a detailed comparison with experimental data would serve no purpose. One comparison can be made with Hall effect measurements above the transition. Lavine<sup>26)</sup> found that the effect in magnetite is so small that it was possible to determine an upper limit only for the Hall coefficient, i.e., a lower limit for the number of carriers. Assuming that only the electrons contribute to the conductivity, Lavine has calculated that the density must be greater than  $10^{21}/cc$ . This is in agreement with the model, which predicts values of  $n_e$  from  $1.54 \times 10^{21}$  at -99° to  $3.66 \times 10^{21}$  at 17°C.

This model is satisfactory as a first and very crude approximation to the band structure of magnetite. The present model is basically similar to the ionic order-disorder picture.

26) L. M. Lavine, Prog. Rep. 26, Cruft Laboratory, Harvard University, Jan., 1953, p. 32.